https://doi.org/10.3311/PPci.23399

Periodica Polytechnica Civil Engineering, 68(4), pp. 1149–1174, 2024

Empirical Punching Shear Capacity Equation for Reinforced Concrete Two-way Slabs with Openings

Ezgi Öztorun Köroğlu[1], Özgür Anil[2*], Muhammad Hatem[3]

[1] Department of Civil Engineering, Cerrahpaşa Faculty of Engineering, Istanbul University, Mahallesi Bağlariçi Caddesi No:7, İstanbul 34320, Türkiye
[2] Department of Civil Engineering, Faculty of Engineering, Gazi University, Celal Bayar Bulvarı, Ankara 06570, Türkiye
[3] Department of Geological Engineering, Faculty of Engineering, Ankara University, Gölbaşı 50. Yıl Yerleşkesi, Ankara 06830, Türkiye
* Corresponding author, e-mail: oanil@gazi.edu.tr

Received: 08 September 2023, Accepted: 05 May 2024, Published online: 24 June 2024

Abstract

This study proposes a new equation to estimate the punching shear capacity of Two Way Reinforced Concrete Flat Slab Column (TRFSC) connections with openings. The TRFSC connections with openings in the literature were simulated using the finite element modeling technique. Then, the test results were used to calibrate and verify the finite element model. Next, the number of test data was artificially increased using the finite element model to cover a wide range of critical perimeters. Finally, the effects of several parameters such as the size of the openings in the reinforced concrete slabs, their position, and distance concerning the column on which the punching loading is applied on the variation of punching shear load capacity of TRFSC connections with openings were observed, the results showed that the proposed equation generally gave better results than the several current code equations. For the study used in the verification of the finite element model, it was observed that the ratios of the punching capacity values calculated using the experimental results and the regulations varied between 0.79 and 0.92 on average, and the regulations gave results that were not on the safe side for TRFSC connections with openings. However, with the nonlinear correction coefficient proposed in this study, the ratios of the experimental results and analytically calculated capacity values were calculated as 1.10 on average, and the standard deviation and variant values decreased much more.

Keywords

two-way RC slab, punching, opening, finite element analysis, ANSYS

1 Introduction

Reinforced concrete flat slab-column systems are one of the most common and conventional structural systems. The benefits of such systems are well known, and they are commonly used in constructing several types of structures (i.e., parking slots, bridge decks, large-scale supermarkets, stores, underground garages, and industrial buildings). The flat slab-column systems offer some benefits, such as short manufacturing periods and reduced costs due to simple formwork arrangements. Moreover, flat slab-column systems generally minimize the floor height causing lower total building height and offering clearer space and lower material cost due to the absence of additional structural elements such as beams and column capitals. Consequently, an extensive study on the design and construction technologies of flat slab-column systems has been performed, providing solid design methods, technical codes, and efficient tools [1–8].

In contrast, flat slab-column connections are vulnerable to a sudden and brittle failure form of punching shear, especially for structures in severe seismic regions. Punching shear failure forms up without any warning signs. A local punching shear failure of a single flat slab-column connection may trigger the progressive punching shear failure of the neighboring connections, which may lead to the collapse of the building. In addition, flat slabs may also have openings for architectural or structural requirements. As known, the size and location of the opening concerning the supporting column are very effective on the punching shear capacity of a flat slab-column system. Accordingly, the effect of openings on the punching shear behavior must be considered carefully. As a result, the accurate estimation of the punching shear capacity of slabs with openings is a major issue.

Cite this article as: Köroğlu, E. Ö., Anil, Ö., Hatem, M. "Empirical Punching Shear Capacity Equation for Reinforced Concrete Two-way Slabs with Openings", Periodica Polytechnica Civil Engineering, 68(4), pp. 1149–1174, 2024. https://doi.org/10.3311/PPci.23399

Various structural design codes [1–4, 9] employ the critical perimeter approach to calculate the punching shear capacity of a slab–column connection for two-way slabs. The critical perimeter approach is mainly based on determining shear stresses caused by vertical loads on a calculated critical slab section around the supporting column. The shear stress is usually calculated as a function of the strength of concrete and the dimensions of the slab and supporting column. Different codes proposed different critical perimeters to calculate the punching shear capacity of the slab. In the study of Elshafey et al. [10], it is stated that equations based on the slab's critical perimeter may yield accurate results when properly formulated.

Furthermore, in the study of Anil et al. [11], it is stated that the equations based on the critical perimeter of the slab yield accurate results for slabs without any openings. Several research studies were conducted to estimate the punching shear capacity of reinforced concrete (RC) slabs using Artificial Neural Networks to increase the accuracy of the punching shear equations [10, 12–15]. It should be noted that studies involving the application of ANN (Artificial Neural Network) to punching shear capacity estimation of RC slabs focused on solid slabs without any openings. In addition, Muttoni [16] proposed a new failure criterion for punching shear based on the rotation of a slab and accurately estimated the punching shear capacities of the flat slabs. The study stated that the punching shear strength of a flat slab depends on the span of the slab rather than on its thickness. However, no information was given in the study about the punching shear capacities of the slabs with openings. Furthermore, Koppitz et al. [17] presented an extensive study on the evaluation of analytical models proposed to estimate the punching shear capacities of RC flat slabs. The models based on rotation-dependent punching shear strength could consider the pre-damage condition that may occur in an existing slab. Moreover, Alam and Amanat [18] studied the effect of flexural reinforcement on the punching shear behavior of reinforced concrete multi-panel flat slabs without any openings. The study stated that the flexural reinforcements embedded in the slab play significant roles in punching shear capacity. Furthermore, an equation including the effect of flexural reinforcement was proposed to calculate the punching shear capacity of flat slabs. The results obtained using the proposed equation were compared with those of nonlinear finite element analyses. It was stated that the results were in good agreement with the finite element analysis results. After a detailed literature review to determine the maximum punching bearing strength values of opening two-way reinforced concrete slabs within the scope of the study, Živković et al. [5]; Pinto et al. [6]; Augustin et al. [7]; Lourenço et al. [8]; Bompa and Onet [19]; Oukaili and Salman [20]; Durucan and Anil [21]; Ha et al. [22]; Ilbegyan et al. [23]; Abduljaleel et al. [24]; Silva et al. [25]; Balomenos et al. [26]; Liberati et al. [27]; Kormosova et al. [28] have been found. After a comprehensive literature review, the limited number of studies listed above were found, examining the effects of openings on the maximum bearing capacity of two-way reinforced concrete slabs under punching loading. However, in these studies, it was not possible to reach a generalizable conclusion for calculating the effects of openings on the punching capacity of slabs. Therefore, establishing an equation for calculating the effects of openings on the punching capacity of slabs is still research subject to be resolved.

On the other hand, as stated before, the size and location of the opening concerning the supporting column are very effective parameters for the punching shear capacity of flat slab-column systems. However, the number of comprehensive studies conducted on the punching shear behavior of flat slab-column systems with openings and without shear reinforcement is very low. An experimental study by Al-Shammari [29] focused on the punching shear behavior of one-way slabs with openings with and without strengthening. The study tested nine specimens, including the specimen without an opening. The results showed that openings decreased the punching shear capacity by 40%. Borges et al. [30] conducted punching shear tests on 13 reinforced concrete flat plates with and without openings or/and shear reinforcement. The openings were adjacent to the shorter sides of rectangular supports and had widths equal to those of the supports. In the study, the methods of calculating punching shear strengths proposed in some codes were reviewed along with some proposed formulations, and their predictions were compared with the test results. It was stated that for small openings, the estimations of codes seem adequate. Oliveira et al. [31] experimentally investigated the punching shear resistance of seven internal reinforced concrete flat slab-column connections, with one hole adjacent to the column, with or without flexural moment transfer of the slab to the column. Test results were compared with the estimations from several code approaches. Then, in the study, a modification of code approaches was proposed to consider the moment caused by the eccentricity at the critical perimeter for slabs with holes. Anil et al. [11] conducted an experimental

study to determine punching shear capacities of the two-way RC flat slab-column (TRFSC) systems with openings. From the results of the experimental study, it is observed that the considered code equations accurately predicted the punching shear capacity of the reference test specimen without any openings. On the contrary, the code equations cannot accurately predict the punching shear capacity of the test specimens having openings.

It is observed that the methods based on the critical perimeter approach, the methods using ANNs, and some other methods (i.e., methods based on the slab rotation) accurately estimated the punching shear capacities of the two-way RC slabs without any openings. On the contrary, similar accuracy is not achieved for two-way RC slabs with openings. Accordingly, this study conducted a series of finite element analyses to propose an accurate yet simple empirical equation for estimating the punching shear capacity of TRFSC systems with openings. In the study, TRFSC specimens tested by Anil et al. [11] are simulated with ANSYS finite element software, and the experimental results are used to calibrate and verify the finite element model. Then, the verified finite element model was used to produce artificial TRFSC systems with openings. Finally, a statistical study was conducted to improve the critical perimeter approach proposed by several structural codes.

As a result of the comprehensive literature review presented in the introduction, it has been seen that most of the studies examining the punching capacities of reinforced concrete slabs have been investigated for slabs without opening. It is stated in the studies in the literature that the capacity calculation equations entered into the regulations generally yield results that are compatible with the experimental results in calculating the slabs' capacities without opening under punching loading, with acceptable low error rates, and on the safe side. However, the literature review showed that the studies examining the effects of openings in reinforced concrete slabs on the punching behavior are extremely few compared to studies examining slabs without openings. However, there are methods in which the openings in the reinforced concrete slabs are taken into account in the equations used in calculating the punching capacity in the regulations. It has been observed that the calculations made using the equations for calculating the effects of openings on the capacities of reinforced concrete slabs under the effect of punching load in the regulations are generally not on the safe side and give inconsistent results with the experimental studies in the literature [5–8, 11, 21, 25, 27]. By using the equations given in the regulations, the punching capacities calculated for reinforced concrete slabs with opening are greater than the results obtained from the experiments and capacity estimates are calculated, which are not on the safe side. It has been observed that a parametric study should be conducted to develop a method different from the equations in the current regulations to calculate the punching capacity of reinforced concrete slabs with openings realistically and follow experimental results. There is not a comprehensive study in the literature on this subject that includes enough parameters to reach generalizable results. For this reason, it is thought that a comprehensive study should be conducted to examine the parameters that are important in the calculation of the punching capacity, such as the size of the openings in the reinforced concrete slabs, their position, and distance concerning the column on which the punching loading is applied.

2 Research significance

The objective of this research study was to develop an equation to accurately estimate the punching shear load carrying capacity of TRFSC systems with openings. As a result of the literature review, it was seen that the capacity calculation equations recommended by the regulations in calculating the punching strength of reinforced concrete slabs with openings were not successful, did not give results compatible with the experimental results, and did not even give results that were on the safe side. For this reason, it is aimed to develop an innovative correction factor that can be used in calculating the punching strength of reinforced concrete slabs with openings, can give results compatible with experimental results, and correct the equations in existing regulations. The procedure followed to develop a new equation representing the punching shear capacity of TRFSC systems with openings consists of five main steps. In the first step, the finite element model that was used to increase the number of data was constructed. In the second step of the study, the finite element model was calibrated using the solid reference test specimen of Anil et al. [11]. The calibrated model was verified in the third step using the eight flat slab-column systems with opening varying sizes and dimensions, tested by Anil et al. [11]. In the fourth step, the number of test data was increased to cover a wide range of opening size and distance to the supporting column, using the calibrated finite element model. Finally, the factors affecting the punching shear load capacity variation were investigated, and their effects were observed. Next, based on

these observations, a new multiplier and power term is implemented into the critical perimeter, which is calculated based on the current code approaches.

3 Experimental study

As stated before, TRFSC connections tested by Anil et al. [11] were used to calibrate and verify the finite element model used in this study. In the study used for the verification of the finite element model, a total of 9 reinforced concrete slab specimens were tested, one of which is a reference element without opening, and the other eight with openings at different positions and sizes. The specimens (2000 × 2000 × 120 mm) were constructed with RC column connections (200 × 200 mm) located at the center of the slab and tested by applying an axial load from the top of the column. In the experimental study, the TRFSC systems were located on simple line supports on the four sides of the slab. The reinforcement details, as well as the dimensions of the specimens, are given in Fig. 1.

Square-shaped openings of two different sizes were left in the experimental specimens tested in the study of Anil et al. [11], and the dimensions of the openings were 300 × 300 mm and 500 × 500 mm, respectively. In addition, another variable examined in the study is the distance of the openings to the column to which punching loading is applied. The openings left in the specimens were positioned in two different ways: adjacent to the column and 300 mm from the column. The openings were also located in parallel and diagonal locations concerning the supporting central column. Locations of the openings on the tested slab are given in Fig. 2.

Properties of the test specimens and compressive concrete strengths are given in Table 1. The compressive strengths of test specimens were measured as 20.35 MPa on average. In the test specimens, ϕ10 tension and compression reinforcements were used and placed in the same ratio in each direction. The ϕ10 tension reinforcements were placed with 175 mm space in each direction, and ϕ10 compression reinforcements were placed with 215 mm space in each direction. Specimen 1 was the test specimen constructed with no opening (used as a reference test specimen). The other eight test specimens were manufactured with openings that vary in size, location, and distance to the column. Compression and tension reinforcements were cut next to the opening in the test specimens, and no other special reinforcement was placed.

4 Finite element modeling

In the study of Anil et al. [11], experimental punching shear load capacities of the test specimens were presented in comparison to punching shear load capacities obtained using several code equations. The comparative results are presented in Table 2. As observed from Table 2, the analytical results obtained using several code approaches yielded accurate or slightly conservative results for the solid reference test specimen. On the contrary, the analytical results for the test specimens with openings are generally inaccurate, staying on the non-conservative side. Based on the observations from the studies of Elshafey et al. [10], Anil et al. [11], Bhatt and Agar [12], and Choi et al. [13], it is clear that the accurate estimation of the punching shear load capacity of the solid RC flat slab-column systems is possible.

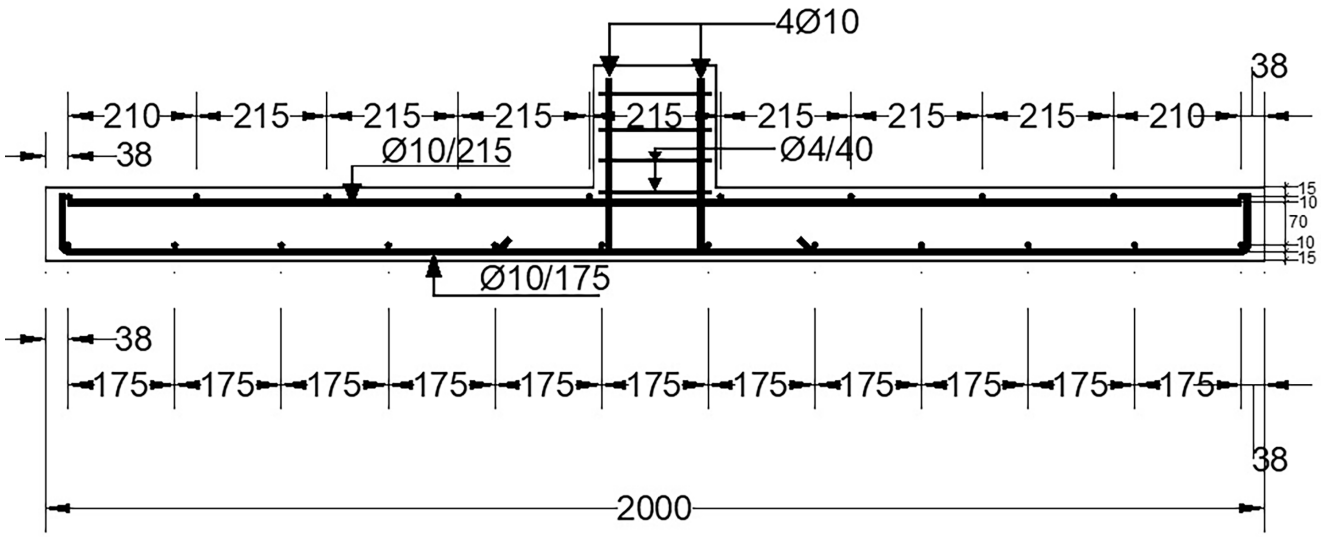

Fig. 1 Reinforcement and dimension of the TRFSC systems considered in this study

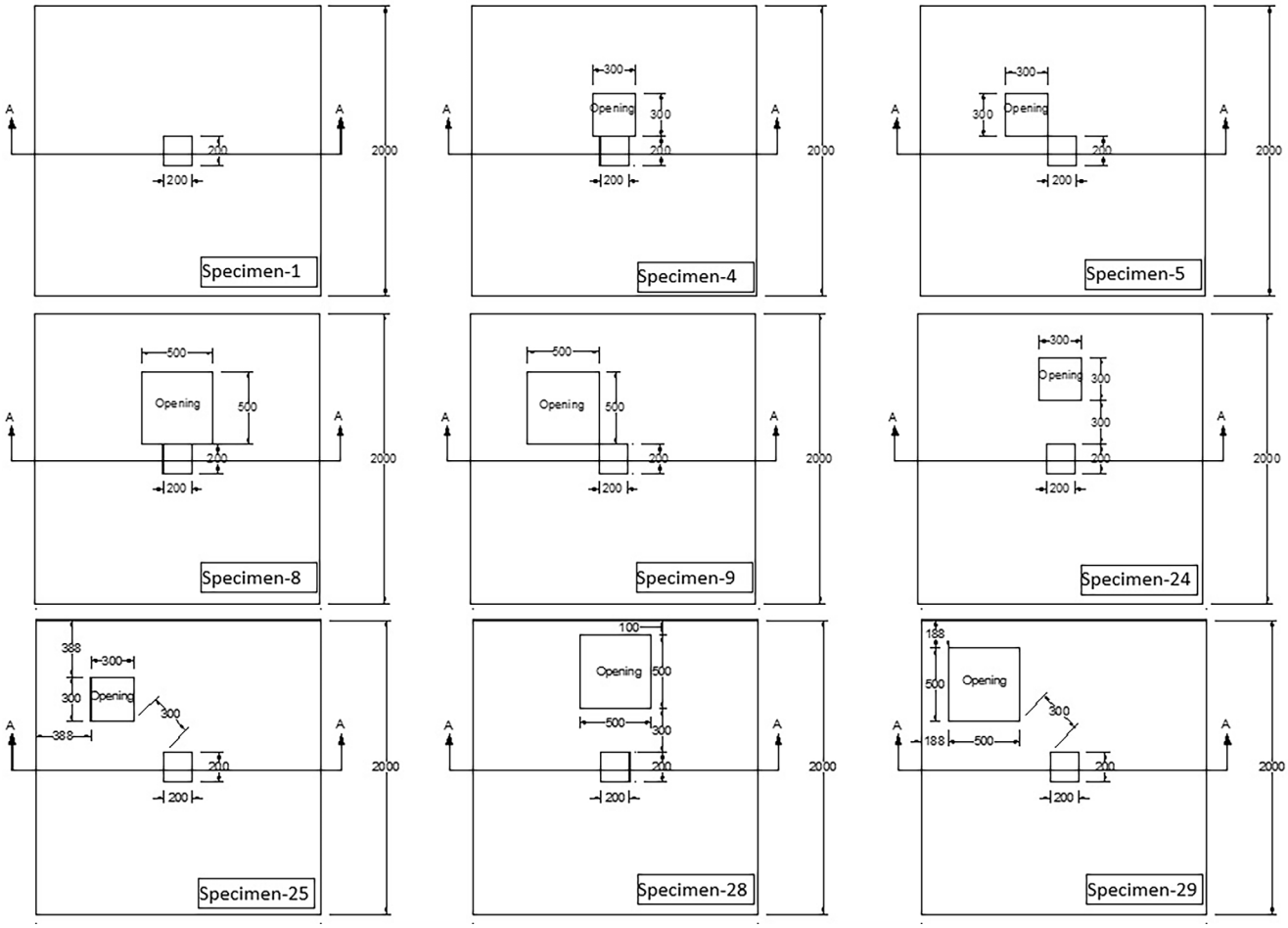

Fig. 2 Layouts of the test specimens considered in this study

Table 1 Properties of test specimens of Anil et al. [11]

Spec. #	Concrete compression strength f'_c (MPa)	Opening	
		Size (mm)	Location concerning the column
1	20.83	Reference (without opening)	
4	20.60	300 × 300	Parallel (adjacent)
5	20.85	300 × 300	Diagonal (adjacent)
8	19.63	500 × 500	Parallel (adjacent)
9	19.61	500 × 500	Diagonal (adjacent)
24	20.02	300 × 300	Parallel (300 mm far)
25	21.24	300 × 300	Diagonal (300 mm far)
28	20.05	500 × 500	Parallel (300 mm far)
29	20.23	500 × 500	Diagonal (300 mm far)

Consequently, in this study, the proposed equation to estimate the punching shear capacity of TRFSC systems is based on the modification of the punching shear load capacity of the solid flat-slab column system. As stated before, in this study, a modification factor was inserted into several current code-mandated equations to estimate the punching shear capacities of RC slab systems with openings. However, the number of relevant and reliable data in the literature is quite limited to conduct a statistical study on the punching shear capacity of two-way RC flat slab-column systems with openings. Accordingly, to observe the effect of location, distance, and size of the openings on the punching shear capacity of TRFSC systems, the nonlinear static finite element analyses of the specimens tested by Anil et al. [11] were performed. Then, the analysis results were used to calibrate and verify the finite element model used to increase the number of test specimens. Consequently, 22 artificial test data were obtained using a verified finite element model of TRFSC systems with openings.

Finite element analyses conducted in this study are performed using the software ANSYS [32]. To simulate the nonlinear behavior of reinforced concrete, a special eight-node element, SOLID65, with extensive modeling capabilities, is used. This solid element is improved primarily for modeling plain and reinforced concrete solids. The most important features of this element are the nonlinear material behavior and its ability to capture the concrete's

Table 2 Experimental punching shear load capacities of the specimens of Anil et al. [11]

Spec. #	Analytical (kN)					Exper. (kN)	Experimental/Analytical capacity					Proposed punching capacity of slab* with the opening (kN)		Experimental/ Proposed capacity	
	TS 500	ACI 318-19	Eurocode 2	JSCE	BS 8110-1:1997		TS 500	ACI 318-19	Eurocode 2	JSCE	BS 8110-1:1997	Linear (Eq. (24))	Nonlinear (Eq. (25))	Linear (Eq. (24))	Nonlinear (Eq. (25))
1	192	181	180	193	169	193	1.01	1.07	1.07	1.00	1.14	-------		-------	
4	127	120	123	129	112	99	0.78	0.83	0.80	0.77	0.88	123	84	0.80	1.18
5	176	166	148	153	138	126	0.72	0.76	0.85	0.82	0.91	148	122	0.85	1.03
8	124	117	109	117	100	77	0.62	0.66	0.71	0.66	0.77	111	68	0.69	1.13
9	170	161	141	148	131	95	0.56	0.59	0.67	0.64	0.73	144	115	0.66	0.83
24	170	161	159	169	151	135	0.79	0.84	0.85	0.80	0.89	150	124	0.90	1.09
25	170	160	162	172	149	172	1.01	1.08	1.06	1.00	1.15	156	136	1.10	1.26
28	159	150	147	156	141	116	0.73	0.77	0.79	0.74	0.82	135	101	0.86	1.15
29	160	151	154	164	142	139	0.87	0.92	0.90	0.85	0.98	150	126	0.93	1.10
Average							0.79	0.83	0.86	0.81	0.92	Average		0.85	1.10
Standard Deviation							0.15	0.16	0.13	0.12	0.14	Standard Deviation		0.13	0.12
Variant (%)							2.14	2.44	1.71	1.46	2.00	Variant (%)		1.69	1.45

* In the calculations made using Eqs. (24) and (25), the punching circumference and slab capacity values without opening of the Eurocode 2 regulation were used.

cracking, crushing, and plastic deformation. In addition, SOLID65 may be used to model solids with reinforcing bars. In the element, three different reinforcements with different orientations may be defined. In this study, reinforcements of the tested slabs are not discretely modeled due to the non-uniform distribution of reinforcement bars located at the top and bottom surfaces of the slabs (Fig. 1). Discrete modeling of reinforcements may lead to many concrete elements (i.e., because of the obligation that the concrete and reinforcement must share the same nodes for composite action) and significantly increase the analysis time. Accordingly, reinforcements of the tested slabs are modeled as smeared in the volume of related concrete elements with specified directions and volume ratios to overcome this difficulty. For the smeared modeling, reinforcement is assumed to have uniaxial stiffness and smeared throughout the volume of the element. Reinforcement input to ANSYS [32] includes material properties, the volumetric ratio of reinforcement to concrete in the element, and the orientation angles of the reinforcement. Consequently, no other additional element is used to simulate the behavior of reinforcement bars. The smeared modeling technique in the ANSYS finite element software is a highly preferred and widely used method for modeling the reinforcement in reinforced concrete elements. When the literature is scanned, it is seen that this technique is still used in studies on this subject. With this technique, the ratio and direction of the reinforcement are defined in the SOLID65 element, where the reinforcement corresponds, without making a change in the location of the reinforcement. In other words, there is no change in the location or useful height of the reinforcement. With this modeling technique, it is possible to define the reinforcement cage very precisely. For this reason, it is still preferred in studies conducted in the literature [33–35].

The behavior of concrete in a linear and nonlinear stage is modeled using linear elastic material properties and multilinear inelastic rate-independent material properties along with the William and Warnke failure criterion [36] for a multi-axial stress state. The William and Warnke failure criterion [36] require uniaxial tensile strength of the concrete and shear transfer coefficients, representing the shear strength reduction factor for concrete across the crack face for the open and closed cases of the crack. The value of the shear transfer coefficient ranges from 0 to 1, with 0 representing a smooth crack and 1 representing a rough crack (i.e., no loss of shear transfer) as stated in ANSYS user's manual [32]. The shear transfer coefficients used in this study are 0.25 for an open crack and 0.75 for a closed crack. Some additional parameters may also be input for the William and Warnke failure criterion [36] for crushing concrete. However, the concrete crushing capability is turned off to avoid known convergence issues, and only the tensile cracking capability of the concrete is used as a failure criterion of the concrete elements to the statement of Kachlakev et al. [37]. Kachlakev et al. [37] stated that compression failure of concrete, which is weak in tension, is improbable due to the secondary tensile strains forming perpendicular to the load [38, 39]. The multilinear isotropic material properties were obtained from a simplified compressive uniaxial stress-strain diagram for concrete, as Desayi and Krishnan [40]. Fig. 3 (a) shows the discrete points of the stress-strain diagram for concrete. The first point represents the linear elastic part of the diagram,

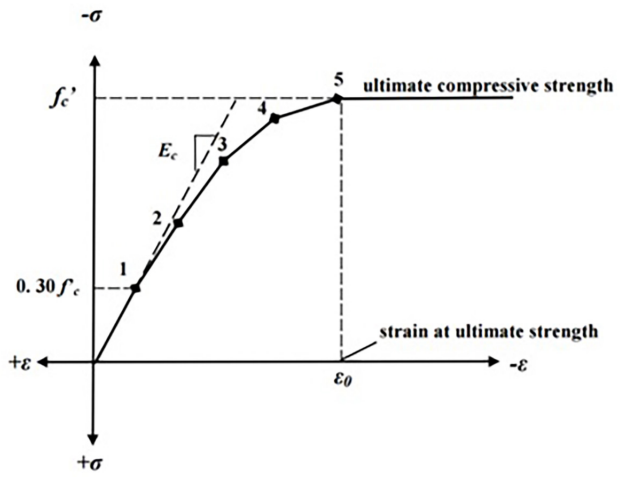

(a)

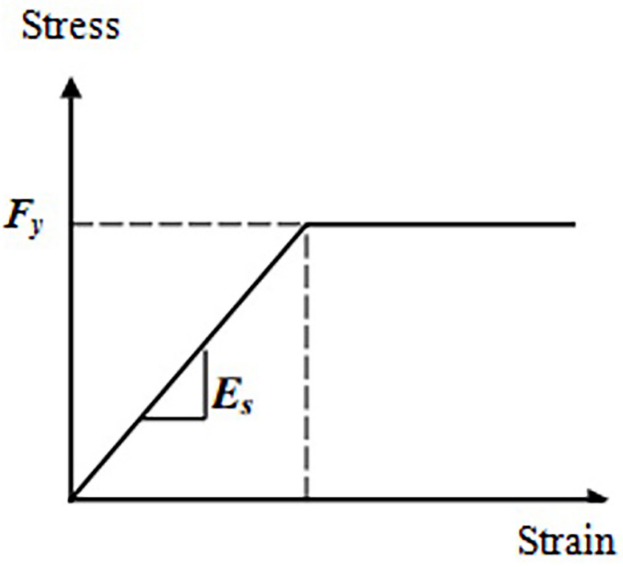

(b)

Fig. 3 Uniaxial stress-strain relationship (a) concrete (b) reinforcement steel

defined as 30% of the ultimate compressive strength. Other points are calculated using the stress-strain relationship for concrete proposed by Desayi and Krishnan [40].

$$f = \frac{E_c \varepsilon}{1 + \left(\frac{\varepsilon}{\varepsilon_0}\right)^2} \tag{1}$$

$$\varepsilon_0 = \frac{2 f_c'}{E_c} \tag{2}$$

In this study, the test specimens of Anil et al. [11] were reproduced and extended using a verified finite element model. In this study, the TRFSC systems were located on simple line supports at the four sides of the slab, and the axial load was applied from the top of a square central column. The test specimens were manufactured using C20 grade (i.e., the ultimate compressive strength of the concrete was 20 MPa) concrete. Furthermore, the tension softening of the concrete (i.e., post-peak stress of the concrete in tension is assumed to be zero) is not simulated. In the experimental study carried out by Anil et al. [11], which was used to verify the finite element model within the scope of the study, the concrete compressive strengths of the test elements were targeted as 20 MPa and the average concrete compressive strengths of the produced test elements were obtained as 20.35 MPa, which is quite close to the targeted value. The compressive strength of the concrete is very low and the tensile strength value of the test elements is also very low, and the peak stress of the concrete in tension value was taken as 1.57 MPa in the numerical analysis. In the numerical analyzes made for the test elements, it is assumed that the maximum tensile capacity value is reached and the tensile bearing capacity is directly zero after this value in the elements where tensile cracks occur, and no material model definition has been made for the reduction in capacity due to any tension softening occurring after the post-peak tensile stress capacity has been reached. It is possible to ignore this effect, since the concrete compressive strength and therefore the tensile strength value is also very small.

Where E_c is the modulus of elasticity of the concrete, ε is the concrete strain, ε_0 is the concrete strain corresponding to the peak concrete stress, and f_c' is the concrete stress. The stress-strain diagram for reinforcement steel is given in Fig. 3 (b). The mechanical properties of the materials used in the test specimens of Anil et al. [11] are given in Table 3 and Table 4 for reinforcement steel and concrete, respectively. The concrete compressive strengths of the test elements are extremely close to each other, and the average concrete compressive strength was calculated as 20.35 MPa. Using this value, the concrete mechanical properties of the numerical analysis models were determined and presented in Table 4. Since the concrete compressive strengths of all test elements were very close to each other, identical concrete material properties were used in the numerical finite element models of all of them. Using the values given in Table 4, multilinear isotropic material properties were obtained from a simplified compressive uniaxial stress-strain diagram for concrete, as Desayi and Krishnan [40] (Fig. 3 (a)).

Table 3 Mechanical properties reinforcement

Yield strength (MPa)	Modulus of elasticity (MPa)	Poisson's ratio
480	200000	0.3

Table 4 Mechanical properties of concrete

Ultimate strength (MPa)		Modulus of elasticity (MPa)	Poisson's ratio
Compressive	Tensile		
20.35	1.57	21000	0.3

On the other hand, the number of elements is an important parameter significantly affecting the computation time and analysis results. Therefore, the model is constructed by using a different number of elements to have a balance between computation time and accuracy. As a first step, the finite element model is built using a very fine mesh with elements having a constant size (25 × 25 × 20 mm). Then as a second step, a similar model is built using elements with varying dimensions (25 × 25 × 20 – 25 × 50 × 20 – 50 × 50 × 20). In the second model (Fig. 4 (a)), the size of the finite element mesh is kept very small (25 × 25 × 20) in the expected punching region located around the column. As the distance from the point where the punching loading is applied, the finite element dimensions are increased (25 × 50 × 20 – 50 × 50 × 20), the number of elements in the model is reduced and the analysis time is shortened. Then the two models are analyzed, and force-displacement relationships are comparatively plotted (Fig. 4 (b)) to observe the difference. From Fig. 4 (b), the difference between the punching shear load capacity is negligibly small (i.e., 2%) concerning the big gain in the analysis time. Besides, support conditions, a sample cracking pattern, stress intensity distribution, and the exaggerated deformed shape of the sample slab are given in Fig. 4 (c)–(f), respectively. Furthermore, Fig. 4 (d)–(f) observed that the cracks and stress intensity distribution agree. The stress and cracks are concentrated on the location of the axial loading and

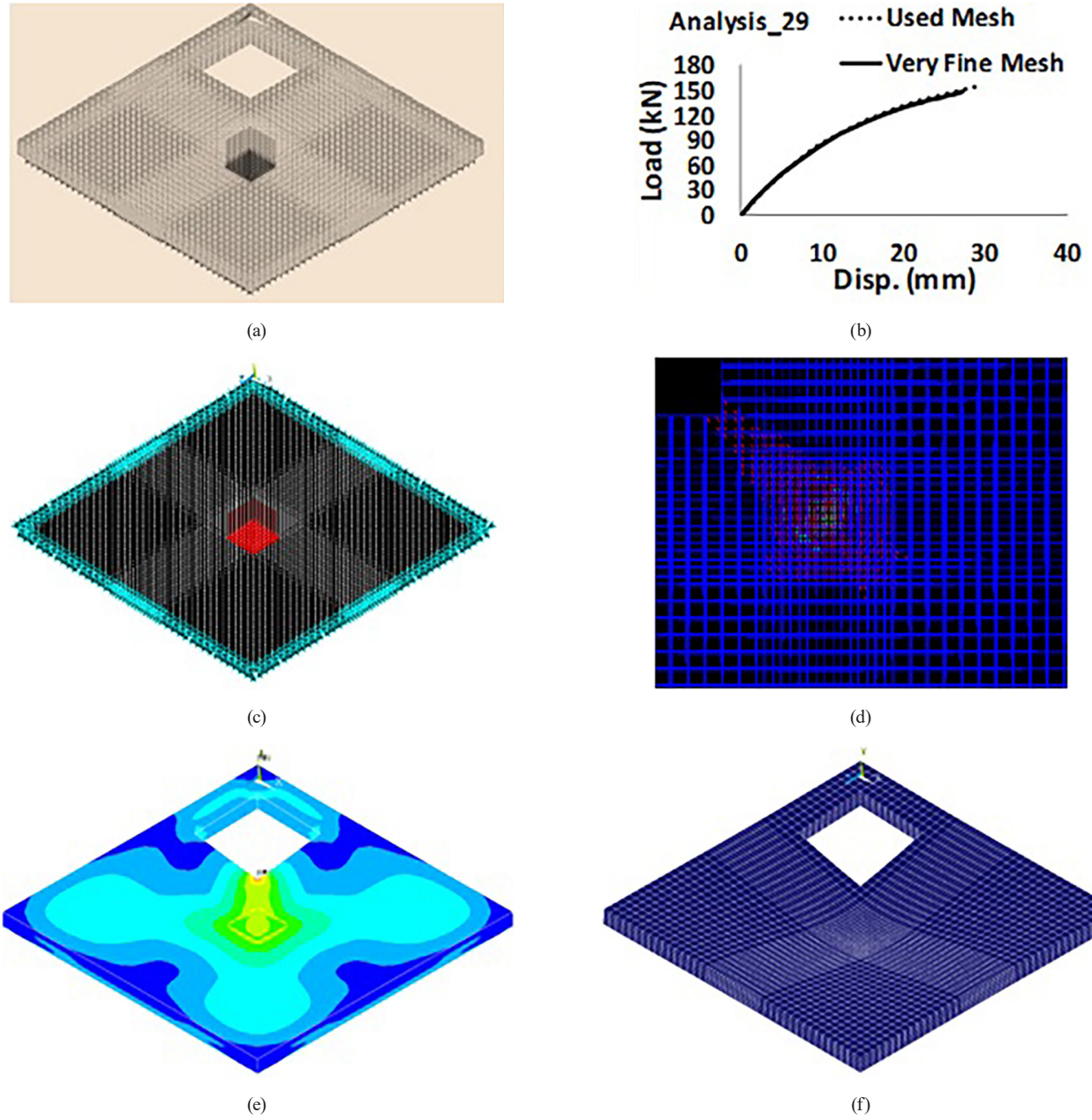

Fig. 4 (a) Finite element model with optimized mesh configuration, (b) load-displacement relationships obtained using regular and optimized mesh configurations, (c) supports along the four edges of the slab, (d) crack distribution, (e) stress intensity distribution on the upper face of the slab, (f) exaggerated deflected shape of the slab

flow through the closest corner of the opening. The damage distributions that occurred as a result of the tests of 9 test elements tested within the scope of the experimental study carried out by Anil et al. [11], and the displacement distributions and stress distributions determined as a result of the analysis of the numerical finite element models are given in Fig. 5 comparatively. When Fig. 5 is examined, it is seen that the displacement and stress distributions obtained as a result of the numerical analyzes and the crack distributions in the tests show great similarities. As a result of the numerical analyzes, the regions where the displacement values are much larger and the stresses are concentrated, and the regions where the cracks and damage are concentrated as a result of the experiments show a great deal of parallelism with each other. This similarity and agreement between the experimental crack distributions and the numerical analysis results is an important indicator that the crack approach used in the numerical analysis model gives very realistic results. When evaluated in terms of the variables examined within the scope of the study, it was seen that as the size of the opening left in the slabs increased, the displacement values obtained as

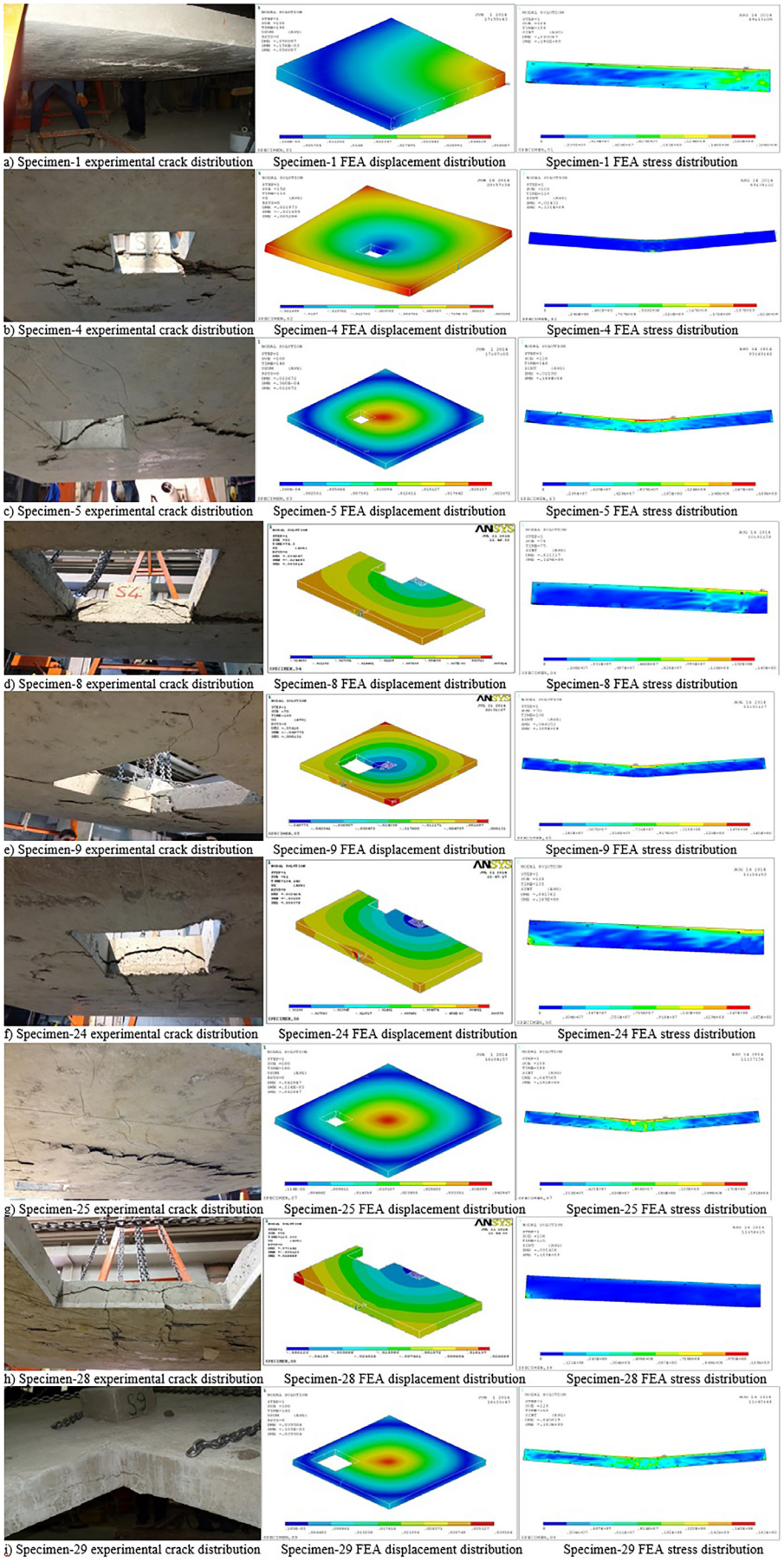

Fig. 5 Comparison of experimental and FEA crack distributions

a result of the numerical analysis also increased and the stress values in the slabs also increased. As a result of the numerical analysis, the position of the opening left in the slabs was much more effective on the displacement and stress distributions in the slabs. The displacements and stresses occurring in the slabs where the opening is positioned parallel to the column where the loading is applied to the slabs have reached much greater values than when the opening is left diagonally to the column. In addition, it has been observed that the area where the stress concentration occurs in slabs where the opening is left adjacent and parallel to the column is larger than in slabs where the opening is left diagonal, and the increase in stresses is distributed over a larger area. When the experimental damage distributions are examined, it is seen that damage distributions that support this result obtained as a result of numerical analysis are obtained. In the specimens where the opening was left parallel and adjacent to the column, the size of the punching cone formed by the punching effect was larger than in the diagonally positioned openings, and the width and number of shear cracks occurring on the inner surface of the opening were larger. It has been observed that as the opening left in the slabs moves away from the column where the punching loading is applied, the displacement values and stress values obtained as a result of the numerical analysis all decrease at large rates, and the size of the area where the stress concentration occurs around the opening decreases. A similar behavioral trend was observed in the experimental damage distributions. The fact that the opening left in the slabs is parallel to the column and on the axis of symmetry has caused the displacement and stress distributions in the slabs to be symmetrical. However, in the slabs where the opening was positioned diagonally, the symmetry in the displacement and stress distributions was disrupted, and the displacements and stresses on the side where the opening was located in the slabs exhibited much larger values.

After determining the mesh size, the nonlinear finite element model was calibrated using the force-displacement relation of the solid reference test specimen of Anil et al. [11]. In the calibration process, the material properties given in Table 4 are used as initial values. The material properties given in Table 4 are modified to account for the bond slip between reinforcement and concrete [41] and the formation of micro-cracks that may occur due to drying shrinkage [42]. The force-displacement relation obtained using the calibrated finite element model is comparatively plotted with that of the specimens of Anil et al. [11] in Fig. 6. The Fig. 6 shows that the stiffness and ultimate punching shear capacity of the analytical model and the experimental study are in good agreement. Consequently, the calibrated finite element model is verified using the TRFSC systems tested by Anil et al. [11]. The displacement and stress distributions obtained after the numerical analyzes for the 9 test elements in the study of Anil et al. [11], which was used to verify the numerical analysis model used within the scope of the study, are given in Fig. 5 in comparison with the damage distributions obtained as a result of the tests. When Fig. 5 is examined, the experimentally obtained damage distributions and the cone fracture geometry occurring on the slab tensile surface as a result of punching are in great agreement with the displacement distributions and stress distributions obtained as a result of the numerical analysis. The load-displacement behaviors determined as a result of experimentally obtained load-displacement graphs and numerical analyzes are given in Fig. 6 for 9 test elements in a comparative way. When Fig. 6 is examined, it is seen that the experimentally measured and numerically calculated initial stiffness values for all test elements are highly compatible and completely overlapping. In addition, this compatibility in stiffness was not limited to the initial stiffness, and the experimental stiffness decrease and the stiffness decrease obtained from the numerical analysis were determined to be very compatible and show a similar trend. The maximum bearing capacity values obtained experimentally and the maximum bearing capacity values calculated as a result of numerical analyzes were determined in a very compatible and successful manner with each other. The load-displacement behaviors of the test elements up to the maximum bearing capacity were obtained successfully and in a very compatible way, overlapping with the load-displacement graphs determined as a result of the numerical analysis. Experimental and numerical energy dissipation capacities up to the maximum carrying capacity are also very close to each other. Since it was aimed to determine the maximum bearing capacity in the numerical analysis study, no effort was made to calculate and estimate the decrease in the load-displacement graph after this point. As it is known, since punching failure is a sudden and brittle failure mechanism, it is thought that it is not necessary to numerically analyze the bearing capacity loss that occurs after the maximum bearing capacity is reached in the slap test elements. Since the punching failure mechanism in reinforced concrete slabs is a very sudden and brittle failure mode, there is a great decrease

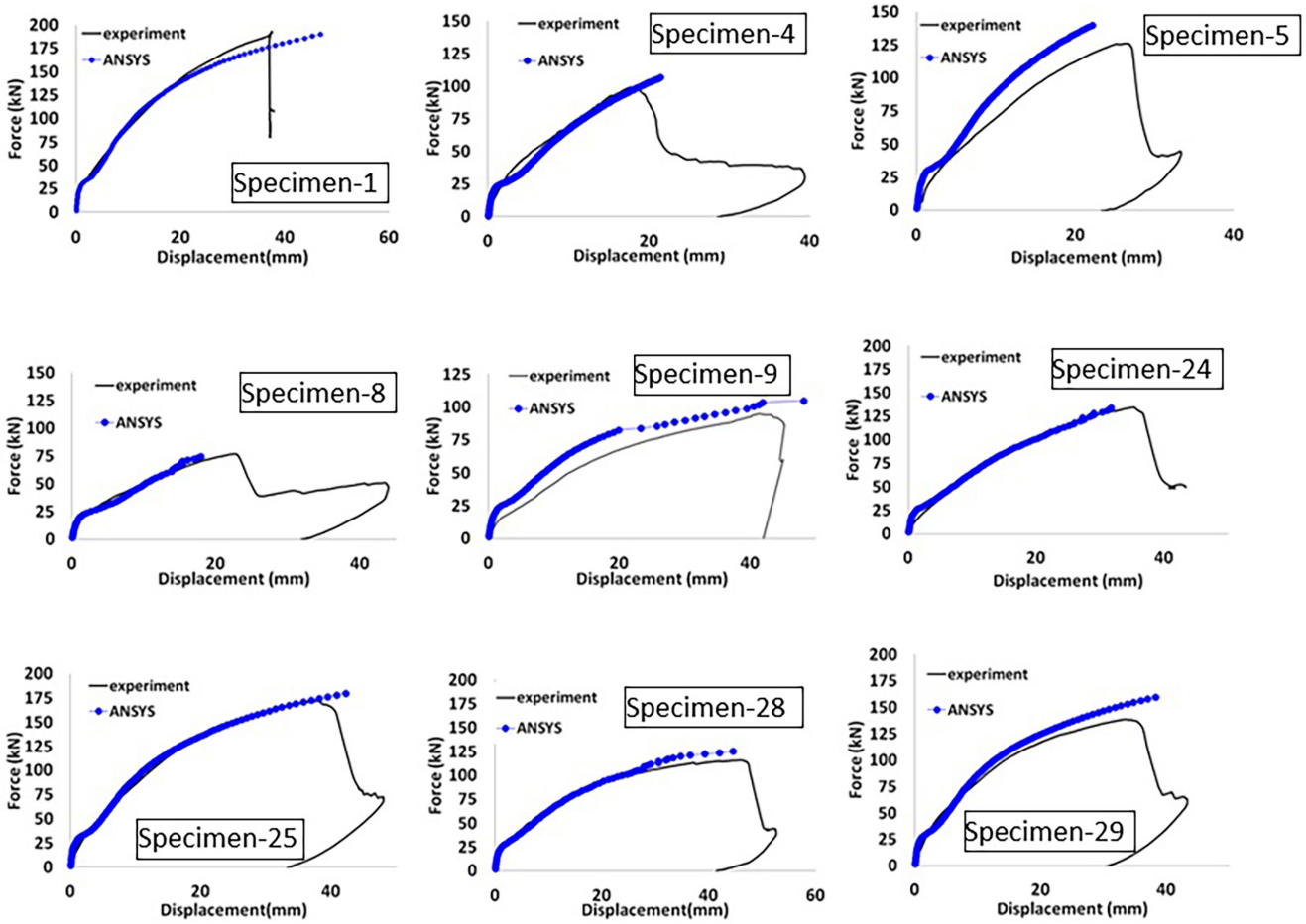

Fig. 6 Comparative load-displacement plot obtained using the finite element model and experimental study

in the bearing capacity after the maximum bearing capacity and a sudden large increase in the displacement value occurs. For this reason, when the literature is examined, it is seen that in many numerical studies in which punching analyzes are performed, only the load-displacement behavior up to the maximum bearing capacity is focused. In this study, the numerical analysis study focused on the parts of the load-displacement graphs where the maximum bearing capacity was reached [43].

As stated before, Anil et al. [11] test specimens contain openings that vary in size and distance to the column. In Fig. 2 and Table 1, the properties of test specimens are given in detail. As stated before, in the scope of this study, only punching shear load carrying capacities of the TRFSC systems are considered. The comparative load-displacement plots from the verification analyses are given in Fig. 6. In Fig. 7, the test specimens' finite element analysis and experimental results are presented comparatively in terms of punching shear load carrying capacities. The Fig. 7 clearly shows that the results obtained using the nonlinear finite element analyses and experimental results are in good agreement. The numerical capacity

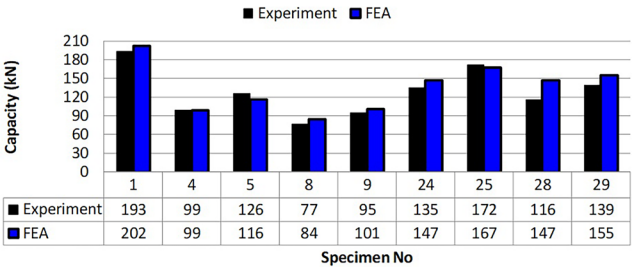

	1	4	5	8	9	24	25	28	29
Experiment	193	99	126	77	95	135	172	116	139
FEA	202	99	116	84	101	147	167	147	155

Fig. 7 Verification results of the finite element model of ultimate load capacity

values and experimental capacity results obtained as a result of the finite element analysis performed on nine reinforced concrete slab test elements, the experimental study of which was carried out by one of the authors (Anil et al. [11]), are presented in Fig. 7. When these values were examined, it was calculated that the average difference between the maximum punching capacity values obtained as a result of the experimental and numerical analysis was 9%, the variation value was 51 kN, and the standard deviation value was 7 kN. Accordingly, the calibrated and verified finite element model is used to produce additional artificial TRFSC systems having openings that vary in size and location.

The number of experimental data is increased using the verified finite element model to cover a wide range of opening dimensions and opening distance to the supporting column (Fig. 8 (a)). The solid rectangles in Fig. 8 (a) represent the supporting column, and the hollow rectangles represent the openings on the slabs. In Fig. 8 (b), the location, size, and distance of the opening from the supporting column are presented, along with the specimen number.

5 Factors affecting the punching shear capacity of two-way RC flat slab-column systems with openings

The analytical study in this section was carried out using all 31 reinforced concrete slabs, including 22 untested reinforced concrete slabs that were analyzed numerically by computer simulation using the verified finite element model using the 9 test specimens tested in the experimental study. It has been tried to establish a connection between the punching capacities of the experimentally tested specimens and the size of the opening in the slab, the distance of the opening to the center of gravity of the column, and the critical punching perimeter, which are effective on the punching carrying capacity. First of all, an analysis of the analytical punching capacity equations in the regulations for 31 reinforced concrete slabs created within the scope of the study is presented in this section. In addition, how to calculate the critical punching perimeters used in calculating the effects of the openings in the slabs on the punching capacity is also examined in this section.

The equations given in TS 500 [1] for the punching load-carrying capacity of the slabs are given in Eqs. (3)–(5). The punching circumference given in the equations was affected by the size of the opening, its position, and the distance to the column. The punching circumference is calculated using the perimeter of the rectangle at a distance of $d/2$ (d: effective slab thickness) from the column surface. The TS 500's [1] approach to the punching circumference is given in Fig. 9 (a).

$$V_{pr} = \gamma f_{ctd} u_p d \tag{3}$$

$$f_{ctd} = 0.35\left(f_{ck}\right)^{1/2} \tag{4}$$

$$\gamma = 1.0 \ \left(\text{In case of axial load}\right) \tag{5}$$

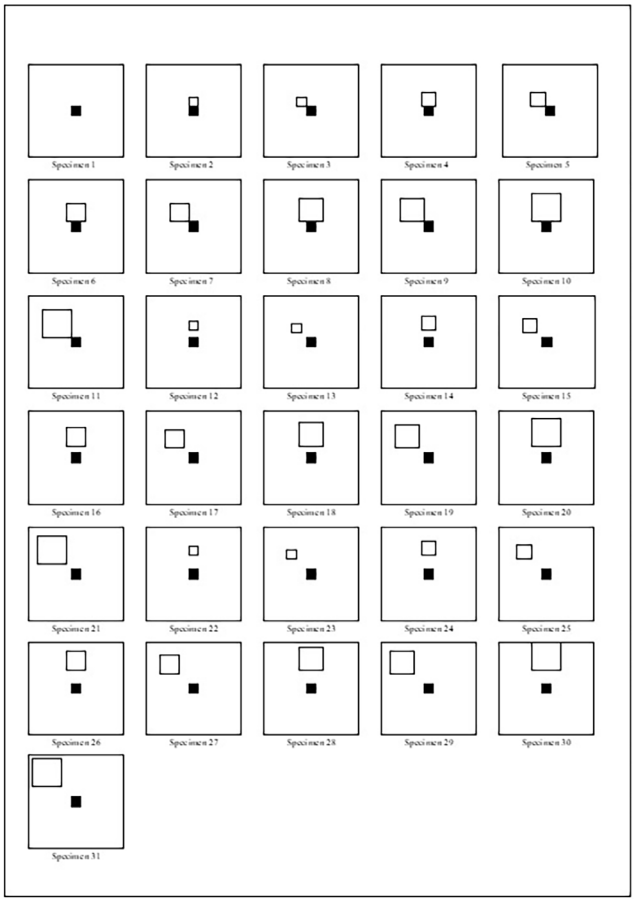

(a)

Spec.#	Opening		
	Size (mm)	Location	Distance (mm)
1 *	Reference		
2	200x200	Parallel	0
3	200x200	Diagonal	0
4 *	**300x300**	**Parallel**	**0**
5 *	**300x300**	**Diagonal**	**0**
6	400x400	Parallel	0
7	400x400	Diagonal	0
8 *	**500x500**	**Parallel**	**0**
9 *	**500x500**	**Diagonal**	**0**
10	600x600	Parallel	0
11	600x600	Diagonal	0
12	200x200	Parallel	150
13	200x200	Diagonal	150
14	300x300	Parallel	150
15	300x300	Diagonal	150
16	400x400	Parallel	150
17	400x400	Diagonal	150
18	500x500	Parallel	150
19	500x500	Diagonal	150
20	600x600	Parallel	150
21	600x600	Diagonal	150
22	200x200	Parallel	300
23	200x200	Diagonal	300
24*	**300x300**	**Parallel**	**300**
25*	**300x300**	**Diagonal**	**300**
26	400x400	Parallel	300
27	400x400	Diagonal	300
28*	**500x500**	**Parallel**	**300**
29*	**500x500**	**Diagonal**	**300**
30	600x600	Parallel	300
31	600x600	Diagonal	300

*These slabs are tested experimentally.

(b)

Fig. 8 Representation of the two-way RC flat slab-column systems (a) top view (b) list

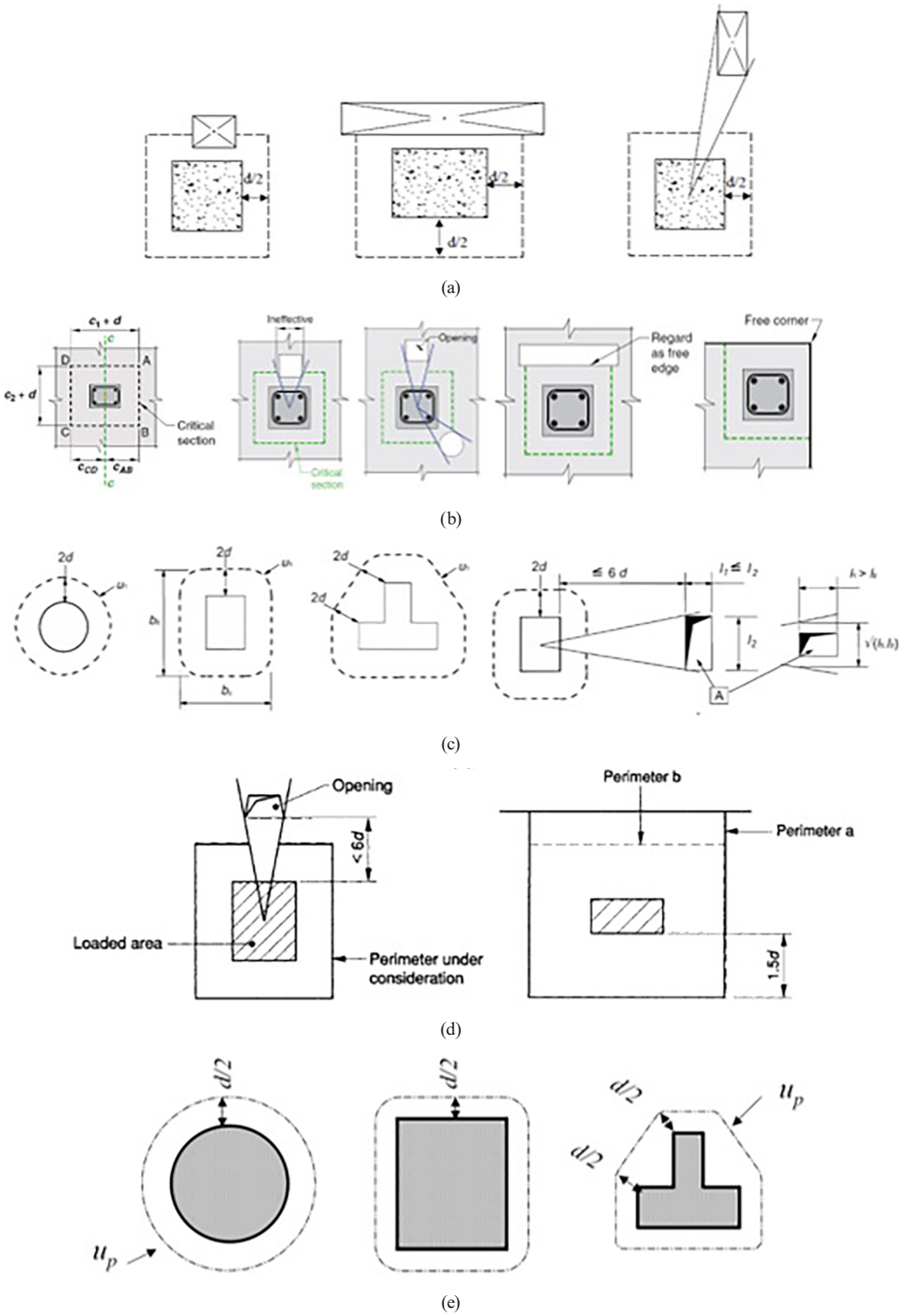

Fig. 9 Punching circumference calculation approach of (a) TS 500 [1], (b) ACI 318-19 [4], (c) Eurocode 2 [2], (d) BS 8110-1:1997 [9], and (e) JSCE [3]

In the equations, V_{pr} is given as the punching load-carrying capacity of the slab, γ as a coefficient representing the bending effect, f_{ctd} as the design axial tensile strength of concrete, and f_{ck} as the characteristic compressive strength of the concrete.

The equations used to calculate the punching load-carrying capacity of slabs in the ACI 318-19 [4] regulation are given in Eqs. (6)–(9). The smallest value calculated from these equations is accepted as the punching capacity. As seen in Fig. 9 (b), in ACI 318-19 [4], similar to TS 500 [1], the existence of the opening is used when calculating the punching circumference. The calculation method of critical punching perimeter is similar to the TS 500 regulation.

$$V_{C,1} = 0.17\left(1+\frac{2}{\beta_c}\right)\lambda\left(f_c'\right)^{1/2} du_p \tag{6}$$

$$V_{C,2} = 0.083\left[\left(\alpha_s d/u_p\right)+2\right]\lambda\left(f_c'\right)^{1/2} du_p \tag{7}$$

$$V_{C,3} = 0.33\lambda\left(f_c'\right)^{1/2} du_p \tag{8}$$

$$\lambda = 1.0 \ \left(\text{In case of axial load}\right) \tag{9}$$

In the equations, V_c is the punching strength provided by the concrete, β is the ratio of the long side of the slab to the short side, λ is a coefficient representing the bending effect, f_c is the compressive strength of the concrete, u_p is the perimeter of the critical section, d is the distance of the upper surface of the slab to the center of the bending reinforcement, α_s represent a coefficient that changes as 40, 30, and 20, respectively, in case it is an inner, edge and corner column or not.

Equations (10)–(13) is proposed to calculate the punching capacity of slabs in the Eurocode 2 [2] regulation. The Eurocode 2 approach to the punching perimeter is given in Fig. 9 (c).

$$V_C = C_{rd,c}k\left(100\rho_l f_{ck}\right)^{1/3} du_p \tag{10}$$

$$C_{rd,c} = 0.18 \tag{11}$$

$$k = 1+\left(\frac{200}{d}\right)^{1/2} \le 2 \ \left(\text{The unit of } d \text{ is mm.}\right) \tag{12}$$

$$\rho_l = \sqrt{\rho_{ly}\rho_{lz}} \tag{13}$$

V_C is the strength of shear stress in the punching circumference, d is the useful slab height, u_p is the punching circumference, f_{ck} is the concrete characteristic compressive strength, ρ_{ly} and ρ_{lz} is defined as the slab tension reinforcement ratio in both directions.

Equations (14)–(16) is proposed for calculating the punching capacity of slabs in the BS 8110-1:1997 [9] regulation. In BS 8110-1:1997 [9], the punching perimeter approach shown in Fig. 9 (d) is used to reflect the effects of openings found in the slabs.

$$V_C = 0.27k\left(100\rho_l f_{c,\text{cube}}\right)^{1/3} du_p \tag{14}$$

$$k = \left(\frac{400}{d}\right)^{1/4} \le 2 \ \left(\text{The unit of } d \text{ is mm.}\right) \tag{15}$$

$$\rho_l \le 0.03 \tag{16}$$

V_C given in the equations represents the punching strength of the flat slab, ρ_l represents the average of the longitudinal reinforcement ratios in both directions in the slab, u_p represents the perimeter of the section to be punched, and d represents the useful height of the slab.

Equations (17)–(21) is proposed for calculating the punching capacity of slabs in the JSCE, 2007 [3] regulation. In JSCE [3], the punching perimeter approach is shown in Fig. 9 (e) and is used to reflect the effects of openings found in the slabs.

$$V_{pr} = 0.1888\beta_d\beta_p\beta_r k\sqrt{f_c}\, du_p \tag{17}$$

$$f'_{pcd} = 0.20\times\sqrt{f'_{cd}} \ \left(\text{N/mm}^2\right), \quad \text{where } f'_{pcd} \le 1.2 \text{ N/mm}^2 \tag{18}$$

$$\beta_d = \sqrt[4]{1000\times d} \ \left(d = \text{mm}\right), \quad \text{when } \beta_d > 1.5 \ \beta_d \text{ is taken as 1.5.} \tag{19}$$

$$\beta_p = \sqrt[3]{100\times p} \text{ when } \beta_p > 1.5 \ \beta_p \text{ is taken as 1.5.} \tag{20}$$

$$\beta_r = 1+1\Big/\left(1+0.25\times\frac{u}{d}\right) \tag{21}$$

V_{pr} given in the equations represents the punching strength of the flat slab, f'_{pcd} represents the compressive design strength of concrete (N/mm^2), u represents the peripheral length of loaded area, u_p represents the perimeter of the section to be punched, d and p represent the effective depth and reinforcement ratio defined as the average values for the reinforcement in two directions, and γ_b represent the member factor and generally be taken as 1.3.

The critical punching perimeter values calculated for a total of 31 reinforced concrete slabs, including nine reinforced concrete slabs tested experimentally and 22 reinforced concrete slabs derived from the finite element model produced using the experimental results, are presented in Table 5. In addition, in Table 5, the critical punching perimeters of the specimens with opening are proportioned to the critical punching perimeter of Specimen-1 without opening, and the dimensionless critical punching circumference ratio values are given. The changes in the critical punching perimeter ratios calculated according to different regulations and presented in Table 5 according to the punching capacity ratios are given in Fig. 10. Punching capacity ratios are dimensionless ratios calculated by the punching capacity values of slabs with opening to the punching capacity of Specimen-1 without opening, just like the critical punching perimeter ratios. In the graphs given in Fig. 10, the variation of the critical punching

Table 5 Critical punching perimeters and critical punching perimeter ratios of all reinforced concrete slabs are calculated according to regulations

Spec. #	Critical punching perimeters (mm)				Critical punching perimeters ratio			
	TS 500 & ACI	Eurocode 2	BS 8110-1:1997	JSCE	TS 500 & ACI	Eurocode 2	BS 8110-1:1997	JSCE
1	1240	2182	2120	1114	1.00	1.00	1.00	1.00
2	930	1637	1590	836	0.75	0.75	0.75	0.75
3	1033	1850	1767	936	0.83	0.85	0.83	0.84
4	827	1495	1413	757	0.67	0.69	0.67	0.68
5	1008	1798	1723	911	0.81	0.82	0.81	0.82
6	775	1405	1325	707	0.63	0.64	0.63	0.63
7	992	1765	1696	896	0.80	0.81	0.80	0.80
8	744	1346	1272	677	0.60	0.62	0.60	0.61
9	982	1743	1678	886	0.79	0.80	0.79	0.80
10	723	1304	1237	657	0.58	0.60	0.58	0.59
11	974	1728	1666	878	0.79	0.79	0.79	0.79
12	1116	1928	1908	994	0.90	0.88	0.90	0.89
13	1087	1955	1859	988	0.88	0.90	0.88	0.89
14	1054	1813	1802	934	0.85	0.83	0.85	0.84
15	1056	1896	1806	958	0.85	0.87	0.85	0.86
16	992	1717	1696	878	0.80	0.79	0.80	0.79
17	1035	1854	1770	938	0.83	0.85	0.83	0.84
18	930	1637	1590	836	0.75	0.75	0.75	0.75
19	1020	1824	1745	923	0.82	0.84	0.82	0.83
20	878	1571	1502	801	0.71	0.72	0.71	0.72
21	1009	1800	1725	912	0.81	0.82	0.81	0.82
22	1164	2022	1988	1020	0.94	0.93	0.94	0.92
23	1119	2011	1912	1018	0.90	0.92	0.90	0.91
24	1124	1943	1921	1002	0.91	0.89	0.91	0.90
25	1088	1956	1860	989	0.88	0.90	0.88	0.89
26	1085	1868	1855	964	0.88	0.86	0.88	0.87
27	1066	1915	1822	967	0.86	0.88	0.86	0.87
28	1046	1800	1789	927	0.84	0.82	0.84	0.83
29	1049	1882	1794	951	0.85	0.86	0.85	0.85
30	1008	1739	1723	891	0.81	0.80	0.81	0.80
31	1036	1856	1771	938	0.84	0.85	0.84	0.84

perimeter ratios according to the punching capacity ratios for each regulation for a total of 31 reinforced concrete slab specimens tested and derived within the scope of the study can be seen. Critical punching perimeter ratio values of TS 500 [1] and ACI 318-19 [4] regulations are shown in the same chart as they are the same. In Fig. 10, the critical punching perimeter change defined in the regulations is shown with the dashed line. Fig. 10 shows the equations that give the relationship between the solid line and the exponential function drawn using 31 results for each regulation and the critical punching perimeter ratios fitted with the punching capacity ratios.

The punching capacity, punching capacity ratios, and critical punching perimeter ratios calculated according to TS 500 [1] and ACI 318-19 [4] regulations for 31 reinforced concrete slabs used as data within the scope of the study are given in Table 6. The graph drawn using the values of critical punching perimeter ratios and punching capacity ratios given in Table 6 is presented in Fig. 11. In Fig. 11, the function that defines the relationship between critical punching circumference ratios and punching capacity ratios is defined as the F_1 function and is given in Eq. (22) below. The F_1 function is a function obtained from the graph given in Fig. 11 and drawn using the critical

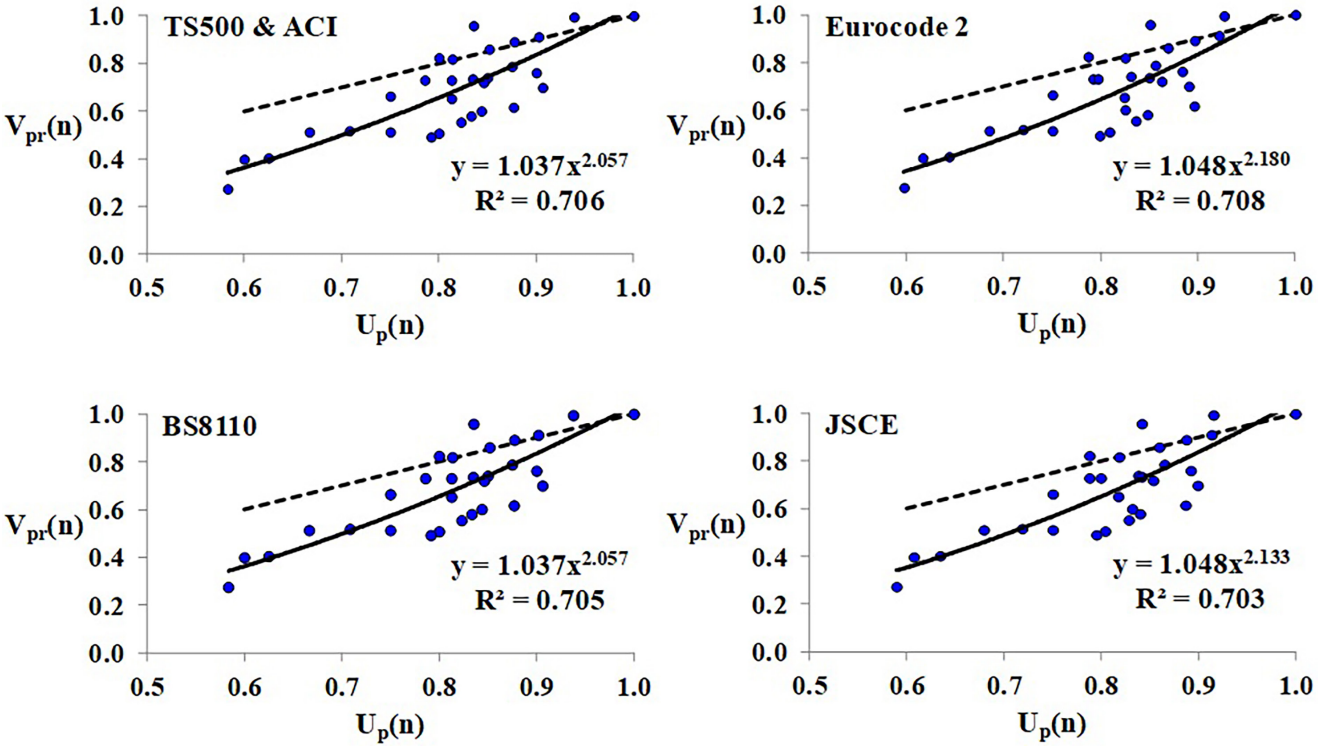

Fig. 10 Relation between the normalized punching shear capacity of TRFSC connections and the normalized critical perimeter (solid line: proposed, dashed line: current code approach)

punching circumference calculated for 31 reinforced concrete slabs, which constitute the data within the scope of the study in Table 6. The equation of the trend line added to the data points in the graph given in Fig. 11 has been determined as the F_1 function. The x coordinates of the data points in the graph drawn in Fig. 11 are the critical punching circumference ratio, and the y coordinates are the punching capacity ratio values made dimensionless by proportioning the critical punching circumference and punching bearing capacity values of the reinforced concrete slabs with opening to the reference reinforced concrete slab critical punching circumference and punching capacity without opening. By adding the trend line to the graph drawn in this way, this power trend line function is obtained as the F_1 function.

$$F_1 = 1.06 \times X^{2.08} \tag{22}$$

The X variable defined within the scope of the study and given in Eq. (22) is not the critical punching perimeter. This value is the normalized, dimensionless critical punching perimeter ratio value. In normalizing this value, the critical punching perimeter of the solid slab without opening, which has the same properties as the slab with openings, was used. The X variable is a dimensionless variable and is calculated by dividing the critical punching perimeter of the slab with opening to the critical punching perimeter of the solid slab with the same properties. After this stage, the effect of the opening area on the variation of punching shear capacity is investigated. To observe the effect of the opening area, the effect of the critical perimeter, which is widely used in many structural codes, on the punching shear load capacity is decoupled from the response. For this purpose, the relation between critical punching perimeter ratio and punching load capacity ratio is obtained, a minimum least square fit regression is performed, and the resulting function F_1 is given in Eq. (22). This equation is used to obtain the punching load-carrying capacities of the TRFSC systems. A new dimensionless parameter, R_1, is obtained by normalizing the punching load capacity ratio using F_1. A new dimensionless parameter, R_1, is given in Eq. (23).

$$R_1 = \frac{\text{Punching Capacity Ratio}}{F_1} \tag{23}$$

Subsequently, the data obtained from the above equation is plotted as a function of the opening area and opening distance to the supporting column and given in Fig. 12. Fig. 12 shows no clear relation between R_1 (dimensionless parameter obtained by decoupling the effect of the critical perimeter ratio from the response) and the opening area.

Table 6 Punching capacities and capacity ratios of all reinforced concrete slabs within the scope of the study

Spec. #	Opening			Remarks	Punching capacity (kN)	Punching* capacity ratio	Critical** punching perimeter ratio
	Size (mm)	Location	Dist. (mm)				
1	Reference without opening			Experiment	193	1.00	1.00
2	200 × 200	Parallel	0	FEA	128	0.66	0.75
3	200 × 200	Diagonal	0	FEA	112	0.58	0.83
4	300 × 300	Parallel	0	Experiment	99	0.51	0.67
5	300 × 300	Diagonal	0	Experiment	116	0.60	0.81
6	400 × 400	Parallel	0	FEA	78	0.40	0.63
7	400 × 400	Diagonal	0	FEA	98	0.51	0.80
8	500 × 500	Parallel	0	Experiment	84	0.44	0.60
9	500 × 500	Diagonal	0	Experiment	101	0.52	0.79
10	600 × 600	Parallel	0	FEA	53	0.27	0.58
11	600 × 600	Diagonal	0	FEA	141	0.73	0.79
12	200 × 200	Parallel	150	FEA	147	0.76	0.90
13	200 × 200	Diagonal	150	FEA	119	0.62	0.88
14	300 × 300	Parallel	150	FEA	143	0.74	0.85
15	300 × 300	Diagonal	150	FEA	166	0.86	0.85
16	400 × 400	Parallel	150	FEA	159	0.82	0.80
17	400 × 400	Diagonal	150	FEA	142	0.74	0.83
18	500 × 500	Parallel	150	FEA	99	0.51	0.75
19	500 × 500	Diagonal	150	FEA	107	0.55	0.82
20	600 × 600	Parallel	150	FEA	100	0.52	0.71
21	600 × 600	Diagonal	150	FEA	158	0.82	0.81
22	200 × 200	Parallel	300	FEA	192	0.99	0.94
23	200 × 200	Diagonal	300	FEA	176	0.91	0.90
24	300 × 300	Parallel	300	Experiment	147	0.76	0.91
25	300 × 300	Diagonal	300	Experiment	167	0.87	0.88
26	400 × 400	Parallel	300	FEA	152	0.79	0.88
27	400 × 400	Diagonal	300	FEA	199	1.03	0.86
28	500 × 500	Parallel	300	Experiment	148	0.77	0.84
29	500 × 500	Diagonal	300	Experiment	156	0.81	0.85
30	600 × 600	Parallel	300	FEA	141	0.73	0.81
31	600 × 600	Diagonal	300	FEA	185	0.96	0.84

* Punching capacity ratios are calculated by proportioning the capacity value of the specimens with the opening to the specimen without opening.
** Values in this column are calculated according to TS 500 and ACI 318-19 regulations. The approach and equations used in calculating the critical punching perimeter in TS 500 and ACI 318-19 regulations are the same, and the calculation method is given in Fig. 9 (a) and Fig. 9 (b), respectively.

Later, the effect of opening distance to the supporting column on the variation of punching load capacity is investigated. To observe the effect of opening distance to the supporting column, Fig. 13 is plotted in terms of R_1 and opening distance to the supporting column. From Fig. 13, it is observed that there is not a clear relation between R_1 and distance to the column.

As a result of the studies carried out, the effect of normalized critical punching perimeter ratio on the punching load carrying capacity variation is presented in Fig. 10. For this purpose, the critical perimeters of the considered TRFSC connections are calculated based on several code equations (Table 5). The punching shear load carrying capacity and the critical perimeter of the two-way RC flat slab-column connections with openings are normalized using the similar TRFSC connection without any opening (Table 6). Then, one of the relationships obtained using the method proposed by several code equations is plotted (as they all give similar results) in Fig. 11. It is observed that there is a clear relation between normalized

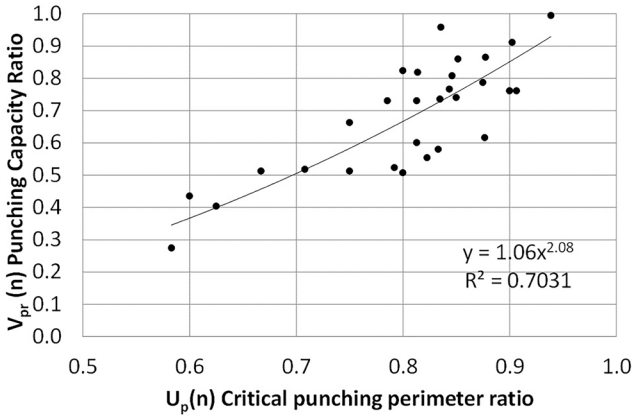

Fig. 11 Variation of normalized punching shear load capacity with normalized critical perimeter

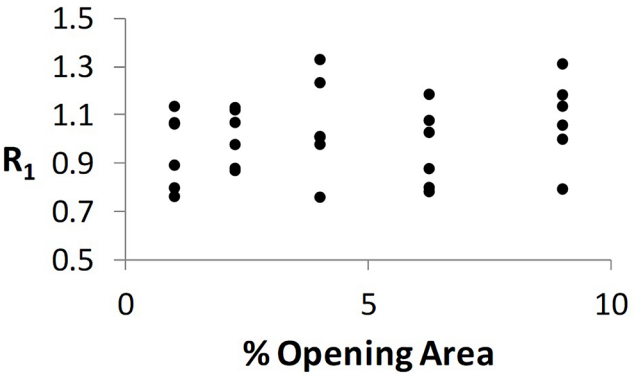

Fig. 12 Variation of R_1 with the opening area

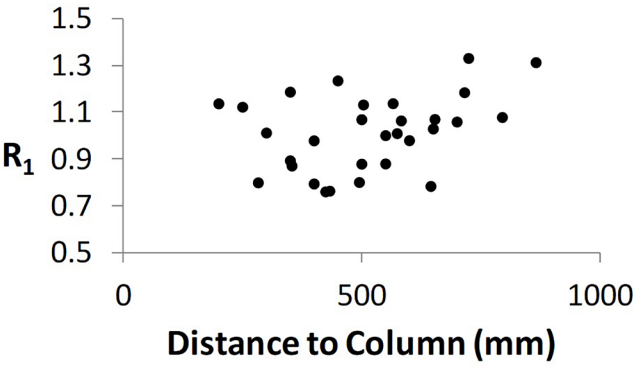

Fig. 13 Variation of R_1 with the opening distance to the supporting column

punching shear capacity ($V_{pr(n)}$ = Punching shear resistance of the slab with opening/Punching shear resistance of the slab without opening) and normalized critical perimeter ($U_{pr(n)}$ = Critical perimeter of the slab with opening/Critical perimeter of the slab without opening).

Consequently, the critical perimeter is used as the variable in developing the proposed equation. As stated above, the parameters affecting the punching capacities of reinforced concrete slabs with openings have been dealt with individually. A relationship between them and their punching capacity has been established. These parameters are the opening size, the distance of the opening to the column where the punching loading is applied, and the critical punching perimeter. As a result of the investigations, the most obvious and consistent relationship with the punching bearing capacity of reinforced concrete slabs with opening could only be established with the critical punching perimeter. For this reason, in this study, it was decided to conduct an equation study using the critical punching perimeter parameter in order to create an equation that can be used in the calculation of the punching bearing capacity of reinforced concrete slabs with opening, which is not complicated, can be more successfully compatible with the experimental results and can give realistic results compared to the calculation methods available in the regulations.

6 Proposed equation

For the proper design of TRFSC connections, simplified but accurate equations are required to estimate the punching shear capacity of such slab-column connections. As stated before, several methods exist to estimate the punching shear capacities of flat-slab column connections without any openings (i.e., structural code provisions and methods based on ANN applications). However, from the recent study conducted by Anil et al. [11], the equations proposed by several structural codes generally overestimate the punching shear capacity of flat slab column connections with openings. Accordingly, this study proposes an equation to estimate the TRFSC systems with openings. The equation is based on scaling the punching shear load capacity of a TRFSC system without any opening. The scaling is achieved by modifying the effect of the calculated critical perimeter of the TRFSC. New factors such as the area of the opening or distance of the opening to the column are not used in the formulation due to their random or negligible effects, as observed in the previous sections, on the variation of punching shear load. In order to examine whether there is a relationship between the punching capacities of the slabs with opening and the critical punching circumference, the necessary calculations were made for 31 slabs within the scope of the study and the F_1 function given in Fig. 11 was obtained. When Fig. 11 is examined, it is seen that there is a significant relationship between the punching capacity of slabs with opening and the critical punching circumference. Then, using the R_1 dimensionless parameter created by using the F_1 function, the other two parameters that affect the punching capacity

of the slabs with opening are the size of the opening and the variation of the distance with respect to the column on which the punching load is applied, in Fig. 12 and Fig. 13, respectively, for the 31 slabs included in the study. When the distributions of the data points in Fig. 12 and Fig. 13 were examined, no significant relationship could be determined between these two parameters and the R_1 function.

In this section, the development of the proposed equation is stated. First, the critical perimeters of the slabs are calculated using the regulations of several structural codes. Then, the punching shear load capacities and the critical perimeters of the TRFSC connections are normalized using those of the solid specimen without any openings. Next, the minimum least square fit of the normalized critical perimeter – normalized punching shear ratio is performed. From the results, it is observed that the best fit is provided using a power function. This observation is based on the value of the coefficient of determination, R_2. For the case of fitting using a power function, the coefficient of determination is calculated as 0.71. This indicates that the proposed equation reasonably estimates 71% of the original punching shear load capacity values. In Fig. 10, the relation between the normalized punching shear capacity of TRFSC connections and the normalized critical perimeter is plotted together with the fitted function (solid line) and the linear functions proposed by current codes (dashed line). The current general form mandated by code equations is given to clarify the form of the proposed equation.

$$V_{\text{opening}} = V_{\text{solid}} \times \left(\frac{U_{\text{opening}}}{U_{\text{solid}}} \right) \text{(linear)} \tag{24}$$

The punching shear capacity of TRFSC systems is proposed to be calculated using:

$$V_{\text{opening}} = V_{\text{solid}} \times \left(\frac{U_{\text{opening}}}{U_{\text{solid}}} \right)^2 \text{(nonlinear)}. \tag{25}$$

Where, V_{solid} and U_{solid} are the punching shear capacity and critical punching perimeter of the slab without any openings. V_{opening} and U_{opening} are the punching shear capacity and critical punching perimeter of the slabs with openings.

This section compares the results obtained using Eq. (25) to those obtained using several code equations. In order to make a fair comparison, the results obtained using code equations are scaled using the punching shear load capacity of the TRFSC connection without any openings. Consequently, it is provided that all code equations exactly predict the experimental punching shear load capacity of the TRFSC connection without any openings. Such scaling is provided to observe the accuracy of the critical perimeter calculation of the structural codes in case of the accurate prediction of the punching load capacity of the TRFSC connection without any openings. The results obtained using the proposed equation (Eq. (25)) and the code-mandated equations are plotted in Fig. 14 for TS 500 [1], Eurocode 2 [2], JSCE [3], ACI 318-19 [4], and BS 8110-1:1997 [9]. The Fig. 14 shows that the proposed equation yielded better results than the conventional code equations for most TRFSC connections. Furthermore, it is observed that the best results are obtained using the critical perimeter calculation method proposed by Eurocode 2 [2] and JSCE [3].

To further assess the accuracy of the proposed equation (Eq. (25)), the experimental results given in the study of Abdul Rasoul [44] were compared with the classical punching shear capacity calculation approach (Eq. (24)) and with the approach proposed in this study (Eq. (25)). The comparative results are given in Fig. 15 in terms of peak punching load capacities. The slabs tested by Abdul Rasoul [44] consist of three slabs with single openings and a solid slab without an opening. In the calculation procedure, the critical punching perimeters are calculated using the Eurocode 2 approach. The Fig. 15 shows that the classical approach yields larger values from the experimental results and the results obtained using the proposed approach.

On the other hand, the proposed approach yields more conservative results than the classical approach for all specimens. However, the results obtained using the proposed approaches are larger than the experimental results for test Specimens 2 and 4. For test Specimen-3 the result obtained using the proposed approach yields a slightly smaller result than the experimental result. The inconsistency in the results may be attributed to the uncertainty of the compressive strength of specimens in the experimental study. In contrast, the compressive strength of the concrete significantly affects the variation of punching load capacity. Such that only the average concrete compressive strengths of the specimens are provided in the experimental study.

Within the scope of the study, the effect of concrete compressive strength on punching behavior was taken into account. Anil et al. [11], while the average concrete compressive strength was around 20 MPa, the equation obtained from the study was also tested and used in Abdul Rasoul [44] study, whose average concrete compressive strength was 70 MPa. In addition, two different studies were added to the study, Lourenço et al. [8] and

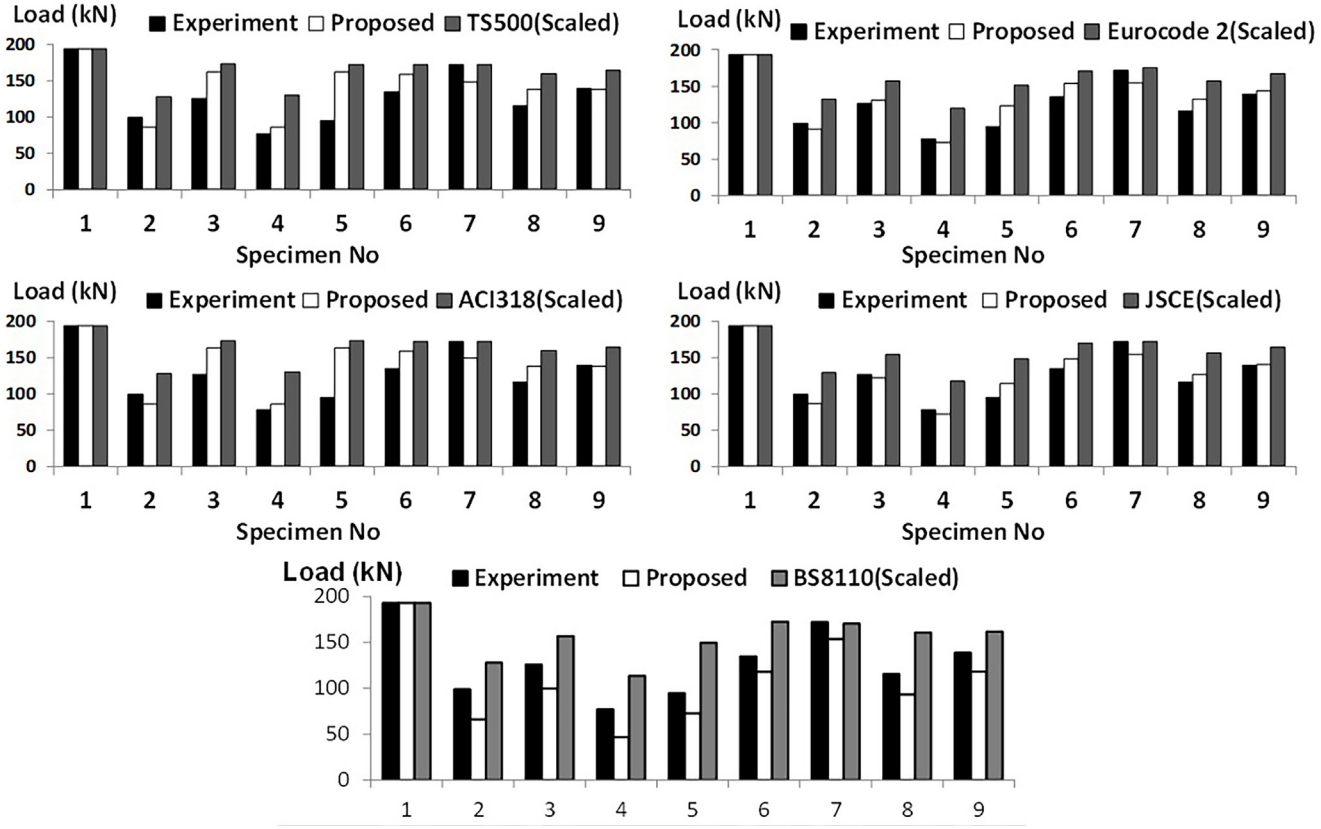

Fig. 14 Results from Anil et al. [11] were obtained using the proposed method, experiment, and several code equations

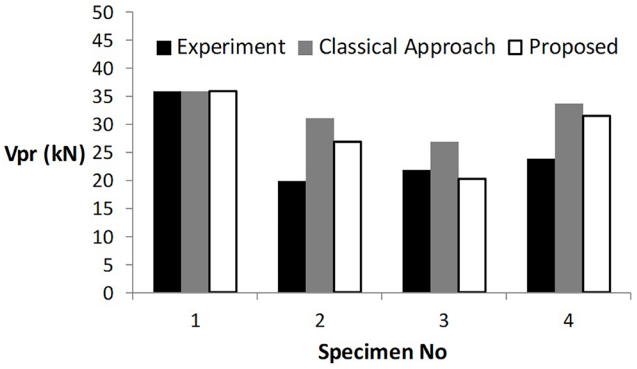

Fig. 15 Comparison of experimental results of Abdul Rasoul [44] with the classical and proposed approaches

Liberati et al. [27], the average compressive strength of concrete was 40 and 45 MPa, respectively. In other words, within the scope of the study, the equation developed on the studies showing variation in concrete compressive strength was used and tested. Within the scope of the study, effective punching circumference was used within the correction coefficient developed in order to improve the punching strength of reinforced concrete slabs with openings and to obtain more realistic and consistent results with the experimental results. This correction coefficient is multiplied by the punching capacity of the slab without opening to calculate the corrected strength of the slab with the opening. Concrete compressive strength is also included in the slab without opening punching capacity equation. It has been statistically seen that the most important parameter affecting the punching capacity of the slabs with the opening is the opening area, which changes due to the opening, and the effective punching circumference, which includes all the effects of the opening position (see Fig. 10 and Fig. 11). A significant relationship between the other parameters and the capacities of the slabs with opening could not be determined statistically. Therefore, the correction coefficient has been developed using the punching circumference only. However, it should not be forgotten that when calculating the capacity of the slabs with openings, the slab capacity without openings should be calculated according to the regulation with the same properties. Then this value should be corrected by multiplying with the correction coefficient suggested in the study. The method developed within the scope of the study can be used to calculate the punching strength of slabs with different concrete compressive strength and reinforcement ratios. The method developed within the scope of the study was tested using the results obtained from four different studies such as Lourenço et al. [8], Anil et al. [11], Liberati et al. [27], and Abdul Rasoul [44]. The concrete

compressive strength and reinforcement ratios of the reinforced concrete slabs tested in these studies are different from each other. Since the calculation method developed in the study was tested using the experimental data used in these studies, it is possible to use it to calculate the punching strength of slabs with different concrete compressive strength and reinforcement ratio. This explanation was added to the article in line with the reviewer's opinion.

Only the effective punching circumference is included in the proposed section for the correction coefficient within the equation proposed for calculating the punching capacity of slabs with openings. There are no other variables in that section. However, as can be seen from the equation with which regulation the calculations will be made, the punching capacity of the slab with opening with identical properties such as concrete compressive strength, reinforcement ratio, and effective slab height should be calculated using that regulation. For example, suppose a calculation is made using the ACI regulation, as stated by the reviewer. In that case, the capacity of the slab without an opening will be calculated by considering the reinforcement ratio. Then the reduced capacity of the slab with an opening will be obtained by multiplying the correction coefficient developed by the authors in the study. However, after extensive research in the literature, very few studies using a similar approach have been found. Aguiar et al. [45] proposed to correct the slab without opening capacity by multiplying it by a coefficient in the equation they developed using a similar approach to the authors. When the correction coefficients are examined, it is seen that only the cmax column maximum width and the bo effective punching circumference are included in the correction coefficient. Aguiar et al. [45] concluded that the most effective parameter on the punching capacity of slabs with openings is the effective punching circumference, as was done by the authors in this study. Within the scope of Aguiar et al.'s [45] study, different correction coefficients have been proposed for different regulations, and a single correction coefficient that can be used for calculating the punching bearing capacity of reinforced concrete slabs with opening has not been proposed as in the scope of the article study.

In order to test the use of Eq. (25) proposed within the scope of the study to calculate the punching capacity of reinforced concrete slabs with opening, two more studies, Lourenço et al. [8] and Liberati et al. [27], were selected from the literature. Liberati et al. [27] conducted an experimental study examining the effects of circular openings left in the slab on the punching capacity, except for the square-shaped openings examined in this study. The punching capacities of Specimen LR without openings and specimens with openings are calculated according to the regulations, and the experimental punching capacities obtained as a result of the tests are presented in Table 7. In Table 7, the ratio of punching circumference with opening/punching circumference without opening recommended in the regulations for standard slabs with opening and capacity ratios calculated with a linear approach is given. Likewise, the capacity ratios calculated with the nonlinear punching circumference ratio equation proposed in Eq. (25), which is proposed within the scope of this study, are given in Table 7. It is seen that the proposed equation for circular openings, in which the suggested results in Table 7 are examined, does not give as successful results as for slabs with square openings. However, as the number of circular openings left in the slabs increased, it was determined that

Table 7 Punching capacities of slabs tested in the study of Liberati et al. [27] according to the recommended equation

Specimen name	Punching capacities according to regulations (kN)			Experimental punching capacity (kN)	Experimental capacity/linear punching capacity equation*			Experimental capacity/proposed nonlinear punching capacity rquation**		
	TS 500	ACI 318-19	Eurocode 2		TS 500	ACI 318-19	Eurocode 2	TS 500	ACI 318-19	Eurocode 2
LR	190.78	179.87	223.03	247.00		-----			------	
LF1	158.55	149.49	167.58	221.00	1.532	1.625	1.301	2.264	1.709	1.709
LF2	185.30	174.71	192.36	250.00	1.471	1.561	1.282	1.460	1.465	1.465
LF3	195.90	184.71	204.05	231.00	1.294	1.373	1.126	1.498	1.203	1.203
LF4	192.22	181.23	218.98	273.00	1.493	1.584	1.278	1.318	1.334	1.334
Average					1.448	1.535	1.244	1.635	1.428	1.428
Standard Deviation					0.091	0.097	0.074	0.369	0.187	0.187
Variant (%)					0.830	0.933	0.554	9.116	2.702	2.702

* The new linear correction coefficient given in Eq. (24), which is recommended to be used in the calculation of the punching capacity developed in the scope of study.

** The new nonlinear correction coefficient given in Eq. (25), which is recommended to be used in the calculation of the punching capacity developed in the scope of study.

the proposed equation gave more successful results and made predictions more compatible with the experimental results. The method proposed within the scope of the study was developed with the data obtained as a result of a parametric finite element analysis validated using experiments of slabs with square opening geometry. However, the success of the developed method was later tested on floors with circular gaps, which were examined experimentally within the scope of the Liberati et al.'s [27] study. The results obtained are given in Table 7, and when examined, acceptable and usable results were obtained.

Experimental data from Lourenço et al.'s [8] study, in which slabs with different concrete compressive strengths were tested, were used to control Eq. (25) proposed in the study. The punching capacities calculated using the regulations and the punching capacities determined as a result of the experiments of a total of four specimens, one of which was tested for reference specimen without opening, is given in Table 8. In addition, the capacity ratios calculated using the linear approach recommended by the regulations and the nonlinear punching circle ratios developed within the scope of this study are also presented in Table 8. When the results obtained as a result of the study are examined, it has been shown that as the concrete compressive strength increases, the success in the values calculated by using Eq. (25), which is recommended for calculating the capacity of the slabs with opening in the study, decreases.

7 Conclusions

This study proposes a new equation to estimate the punching load carrying capacity of the TRFSC (Two Way Reinforced Concrete Flat Slab Column) connections with openings. For this purpose, the TRFSC connections with openings tested by Anil et al. [11] are simulated using the finite element modeling technique. Then, the test results are used to calibrate and verify the constructed finite element model. Next, the number of test data is artificially increased using the finite element model to cover a wide range of critical perimeters. Finally, the effects of several parameters on the variation of punching shear load capacity of TRFSC connections with openings are observed, and a nonlinear factor is introduced to current code equations. The results show that the proposed equation generally performs better than the current code equations. The average values of the ratios of the experimental punching capacities and the capacities obtained with the linear correction coefficient and nonlinear correction coefficient developed within the scope of the study were calculated as 0.85 and 1.10, respectively, and these values are better than those obtained with the current regulations (Table 2). The conclusions deduced from the study are:

- The critical punching perimeter approach is an accurate technique to calculate the punching load capacity of TRFSC connections.
- Variables such as the size of the opening and the distance of the opening to the loaded column, which are tried to be expressed by this result, are not found to be significantly correlated with the punching capacities of the reinforced concrete slabs with opening alone. The analyzes for these variables are presented by graphing in Fig. 12 and Fig. 13, and it is seen that the data are scattered and they do not reveal a significant relationship with the punching capacity of the slabs with opening on their own. However, as it is known, these two variables are the size of the opening and the distance of the opening to the loading

Table 8 Punching capacities of slabs tested in the study of Lourenço et al. [8], according to the recommended equation

Specimen name	Punching capacities according to regulations (kN)			Experimental punching capacity (kN)	Experimental capacity/linear punching capacity equation*			Experimental capacity/proposed nonlinear punching capacity equation**		
	TS 500	ACI 318-19	Eurocode 2		TS 500	ACI 318-19	Eurocode 2	TS 500	ACI 318-19	Eurocode 2
LR-A	194.23	181.10	224.05	249.90		-----			------	
LF1-A	172.28	162.43	217.03	187.60	1.12	1.23	0.99	1.30	1.46	1.18
LF2-A	126.67	119.44	159.65	187.60	1.33	1.48	1.20	1.84	2.11	1.71
LF4-A	80.85	76.23	102.88	184.00	1.44	1.63	1.32	2.19	2.63	2.13
Average					1.30	1.45	1.17	1.78	2.07	1.67
Standard Deviation					0.13	0.17	0.14	0.37	0.48	0.39
Variant (%)					1.77	2.79	1.83	13.42	22.99	15.02

* The new linear correction coefficient given in Eq. (24), which is recommended to be used in the calculation of the punching capacity developed in the scope of study.
** The new nonlinear correction coefficient given in Eq. (25), which is recommended to be used in the calculation of the punching capacity developed in the scope of study.

point, which are effective quantities in calculating the critical punching circumference. As a result of calculating the critical punching circumference by combining these two variables, it was seen that this value has a significant relationship with the punching capacity of reinforced concrete slabs with opening, and a function was obtained by adding a power trend line to this data distribution in Fig. 11. Although the opening size and opening location parameters alone could not find a correlation with the punching capacity of the slabs with opening, a correlation was obtained between the critical punching circumference, which is calculated by combining the two variables, and the punching capacity.

- The punching load capacity of TRFSC connections considered in this study is estimated using the nonlinear form given in Eq. (25), and accurate results are obtained concerning the results obtained using the linear form proposed by current code equations (Eq. (24)). Concerning that, it may be concluded that the variation of punching load carrying capacity for TRFSC connections used in this study is well simulated by introducing a nonlinear term to the classical approach.
- Within the scope of the study, an effort has been made to make the equation as simple as possible, which is proposed as a correction coefficient for the equations used in the calculation of the capacity of the slabs without openings in the standard regulations for the calculation of the punching capacities of the reinforced concrete slabs with the opening. In this study, as in Aguiar et al. [45], a correction coefficient including only the effective punching circumference is suggested. The equation proposed in the study has been checked with the experimental results obtained from the studies in the literature in slabs with circular openings, and the concrete compressive strength varies, and it has been seen that it makes acceptable estimates. Due to the very limited number of studies in the literature on slabs with opening, it is thought that the lack of experimental data makes it difficult to reach a generalizable conclusion on this subject.
- The authors made an effort to use the equation they proposed within the scope of the study they carried out and to be useful to the designers, and compared them with the results of other researchers in the literature. The proposed equation has been tested as much as possible by comparing the results obtained in studies such as Lourenço et al. [8], Liberati et al. [27] and Abdul Rasoul [44]. In addition, a comparison was made with 9 experimental results in the study conducted by Anil et al. [11] by one of the authors, and the number of data was increased from 9 to 31 with a numerical analysis model validated by these results. However, within the scope of this study, this equation has been suggested for the case of a single opening in reinforced concrete slabs.

It should not be forgotten that the new correction coefficients developed within the scope of the study to calculate the punching capacities of reinforced concrete slabs with opening in a way that is more compatible with the experimental results, realistic and on the safe side, were developed for single-opening slabs with square and circular geometry. The developed coefficients were tested for opening size, opening location, distance of the opening to the loading point, and different concrete compressive strengths. However, it is not recommended to use these coefficients for openings with reinforced concrete slabs with more than one opening. It should be noted that the correction coefficient was developed for single-opening slabs in order to calculate the punching capacity of the slabs developed within the scope of this study in a more compatible way with the experimental results. In order to develop the proposed equation for estimating the punching capacity in slabs with multiple opening, studies should be expanded, numerical analyzes should be performed, and a data collection should be created from experimental data with multiple openings by reviewing the literature.

References

[1] TSE "TS 500 Betonarme Yapıların Tasarım ve Yapım Kuralları" (TS 500 Requirements for design and construction of reinforced concrete structures), Türk Standartları Enstitüsü, Ankara, Turkey, 2000. (in Turkish)

[2] CEN "CEN EN 1992-1-1:2004/AC:2010 Eurocode 2: Design of concrete structures - Part 1-1: General rules and rules for buildings, European Committee for Standardization, Brussels, Belgium, 2010.

[3] JSCE "Standard specifications for concrete structures - 2007: Structural performance verification", Japan Society of Civil Engineers, 2007. ISBN 9784810604542

[4] ACI Committee 318 "ACI CODE-318-19(22): Building Code Requirements for Structural Concrete and Commentary (Reapproved 2022)", American Concrete Institute, Farmington Hills, MI, USA, ACI 318-19, 2019. https://doi.org/10.14359/51716937

[5] Živković, S., Bešević, M., Purčar, M. V., Kozarić, L. "Nonlinear finite element analysis of punching shear strength of eccentrically loaded RC flat slabs with opening", KSCE Journal of Civil Engineering, 23(11), pp. 4771–4780, 2019. https://doi.org/10.1007/s12205-019-0075-5

[6] Pinto, V. C., Branco, V., Oliveira, D. R. "Punching in two-way RC flat slabs with openings and L section columns", Engineering Computations, 36(7), pp. 2430–2444, 2019. https://doi.org/10.1108/EC-12-2018-0596

[7] Augustin, T., Fillo, L., Halvonik, J. "Punching resistance of slab-column connections with openings", Structural Concrete, 21(1), pp. 278–290, 2020. https://doi.org/10.1002/suco.201900158

[8] Lourenço, D. D. S., Liberati, E. A. P., Marques, M. G., Almeida, L. C. D., Trautwein, L. M. "Reinforced concrete flat slabs with openings at different distances from the column", Revista IBRACON de Estruturas e Materiais, 14(1), e14111, 2021. https://doi.org/10.1590/s1983-41952021000100011

[9] BSI "BS 8110-1:1997 Structural Use of Concrete - Code of Practice for Design and Construction", British Standards Institution, London, UK, 1997.

[10] Elshafey, A. A., Rizk, E., Marzouk, H., Haddara, M. R. "Prediction of punching shear strength of two-way slabs", Engineering Structures, 33(5), pp. 1742–1753, 2011. https://doi.org/10.1016/j.engstruct.2011.02.013

[11] Anil, Ö., Kina T., Salmani, V. "Effect of opening size and location on punching shear behavior of two-way RC slabs", Magazine of Concrete Research, 66(18), pp. 955–966, 2014. https://doi.org/10.1680/macr.14.00042

[12] Bhatt, P., Agar, T. J. A. "A neural network for predicting the punching shear strength of internal column-flat slab junctions without shear reinforcement", Trita-BKN. Bulletin, 57, pp. 39–46, 2000.

[13] Choi, K.-K., Taha, M. M. R., Sherif, A. G. "Simplified punching shear design method for slab–column connections using fuzzy learning", ACI Structural Journal, 104(4), pp. 438–447, 2007. https://doi.org/10.14359/18774

[14] Choi, S.-H., Lee, D. H., Oh, J.-Y., Kim, K. S., Lee, J.-Y., Shin, M. "Unified equivalent frame method for flat plate slab structures under combined gravity and lateral loads – Part 2: verification", Earthquakes and Structures, 7(5), pp. 735–751, 2014. https://doi.org/10.12989/eas.2014.7.5.735

[15] Kim, K. S., Choi, S.-H., Ju, H., Lee D. H., Lee, J.-Y., Shin, M. "Unified equivalent frame method for flat plate slab structures under combined gravity and lateral loads – Part 1: derivation", Earthquakes and Structures, 7(5), pp. 719–733, 2014. https://doi.org/10.12989/eas.2014.7.5.719

[16] Muttoni A. "Punching Shear Strength of Reinforced Concrete Slabs without Transverse Reinforcement", ACI Structural Journal, 105(4), pp. 440–450, 2008. https://doi.org/10.14359/19858

[17] Koppitz, R., Kenel, A., Keller. T. "Punching shear of RC flat slabs – Review of analytical models for new and strengthening of existing slabs", Engineering Structures, 52, pp. 123–130, 2013. https://doi.org/10.1016/j.engstruct.2013.02.014

[18] Alam, A. K. M. J., Amanat, K. M. "Effect of reinforcement on punching shear of multi-panel flat slab", Journal of Civil Engineering (IEB), 41(2), pp. 123–137, 2013.

[19] Bompa, D. V., Onet, T. "Behaviour of Symmetric Flat-Slab Connections with Openings in the Control Perimeter", Scientific Bulletin Series D: Mining, Mineral Processing, Non-Ferrous Metallurgy, Geology and Environmental Engineering, 24(2), pp. 111–116, 2010.

[20] Oukaili, N. K., Salman, T. S. "Punching shear strength of reinforced concrete flat plates with openings", Journal of Engineering, 20(1), pp. 1–20, 2014. https://doi.org/10.31026/j.eng.2014.01.01

[21] Durucan, C., Anil, Ö. "Effect of opening size and location on the punching shear behaviour of interior slab–column connections strengthened with CFRP strips", Engineering Structures, 105, pp. 22–36, 2015. https://doi.org/10.1016/j.engstruct.2015.09.033

[22] Ha, T., Lee, M.-H., Park, J., Kim, D.-J. "Effects of openings on the punching shear strength of RC flat-plate slabs without shear reinforcement", The Structural Design of Tall and Special Buildings, 24(15), pp. 895–911, 2015. https://doi.org/10.1002/tal.1217

[23] Ilbegyan, S., Ranjbar, M. M., Abdollahi, S. M. "Shear capacity of reinforced concrete flat slabs made with high-strength concrete: A numerical study of the effect of size, location, and shape of the opening", International Journal of Engineering, 30(2), pp. 162–171, 2017. https://doi.org/10.5829/idosi.ije.2017.30.02b.02

[24] Abduljaleel, M. T., Mahmoud, A. S., Yousif, A. R. "Experiential investigation of two-way concrete slabs with openings reinforced with glass fiber reinforced polymer bars", Journal of Engineering Science and Technology, 12(4), pp. 898–912, 2017.

[25] Silva, J. A., Marques, M. G., Trautwein, L. M., Gomes, R. B., Guimarães, G. N. "Punching of reinforced concrete flat slabs with holes and shear reinforcement", REM - International Engineering Journal, 70(4), pp. 407–413, 2017. https://doi.org/10.1590/0370-44672017700022

[26] Balomenos, G. P., Genikomsou, A. S., Polak, M. A. "Investigation of the effect of openings of interior reinforced concrete flat slabs", Structural Concrete, 19(6), pp. 1672–1681, 2018. https://doi.org/10.1002/suco.201700201

[27] Liberati, E. A. P., Marques, M. G., Leonel, E. D., Almeida, L. M., Trautwein, L. M. "Failure analysis of punching in reinforced concrete flat slabs with openings adjacent to the column", Engineering Structures, 182, pp. 331–343, 2019. https://doi.org/10.1016/j.engstruct.2018.11.073

[28] Kormosova, Ľ., Halvonik, J., Majtánová, L. "Safety of the Models for Assessment of Punching Resistance of Flat Slabs with Openings Adjacent to the Columns", Solid State Phenomena, 309, pp. 186–192, 2020. https://doi.org/10.4028/www.scientific.net/SSP.309.186

[29] Al-Shammari, A. H. H. "Effect of openings with or without strengthening on punching shear strength for reinforced concrete flat plates", Journal of Engineering, 17(2), pp. 218–234, 2011. https://doi.org/10.31026/j.eng.2011.02.03

[30] Borges, L. L. J., Melo, G. S., Gomes R. B. "Punching Shear of Reinforced Concrete Flat Plates with Openings", ACI Structural Journal, 110(4), pp. 547–556, 2013.
https://doi.org/10.14359/51685740

[31] Oliveira, D. C., Gomes, R. B., Melo, G. S. "Punching shear in reinforced concrete flat slabs with hole adjacent to the column and moment transfer", Revista IBRACON de Estruturas e Materiais, 7(3), pp. 414–440, 2014.
https://doi.org/10.1590/S1983-41952014000300006

[32] Ansys Inc. "ANSYS® Academic Research (Release 14.5)", [computer program] Ansys, Cannonsburg, PA, USA, 2012.

[33] Dahmani, L., Khennane, A., Kaci, S. "Crack Identification in Reinforced Concrete Beams Using ANSYS Software", Strength of Materials, 42(2), pp. 232–240, 2010.
https://doi.org/10.1007/s11223-010-9212-6

[34] Gherbi, A., Dahmani, L., Boudjemia, A. "Study on Two Way Reinforced Concrete Slab Using ANSYS with Different Boundary Conditions and Loading", International Journal of Civil and Environmental Engineering, 12(12), pp. 1151–1156, 2018.
https://doi.org/10.5281/zenodo.2022689

[35] Hasan, M. A., Amin, A., Riyad, R. H. "Numerical Analysis of Crack Propagation in Beam Supported Reinforced Concrete Two-Way Slab", In: Proceedings of International Exchange and Innovation Conference on Engineering & Sciences (IEICES), Kyushu University, Fukuoka, Japan, vol. 7, 2021, pp. 77–83.
https://doi.org/10.5109/4738569

[36] William, K. J., Warnke, E. P. "Constitutive Model for the Triaxial Behavior of Concrete", IABSE reports of the working commissions = Rapports des commissions de travail AIPC = IVBH Berichte der Arbeitskommissionen, 19, III-1, 1974.
https://doi.org/10.5169/seals-17526

[37] Kachlakev, D., Miller, T., Yim, S., Chansawat, K., Potisuk, T. "Finite Element Modeling of Reinforced Concrete Structures Strengthened with FRP Laminates", Oregon Department of Transportation Research Group, Salem, OR, USA, Federal Highway Administration, Washington, DC, USA, Rep. FHWA-OR-RD-01_XX, 2001.

[38] Mindess, S., Young, J. F. "Concrete", Prentice-Hall, 1981. ISBN 9780131671065

[39] Shah, S. P., Swartz, S. E., Ouyang, C. "Fracture Mechanics of Concrete: Applications of Fracture Mechanics to Concrete, Rock and Other Quasi-Brittle Materials", John Wiley & Sons, 1995. ISBN 978-0-471-30311-4

[40] Desayi, P., Krishnan, S. "Equation for the Stress-Strain Curve of Concrete", ACI Journal Proceedings, 61(3), pp. 345–350, 1964.
https://doi.org/10.14359/7785

[41] Kazaz, I. "Application of Bond-Slip in the Finite Element Analyses of Reinforced Concrete Shear Walls", Pamukkale University Journal of Engineering Sciences, 18(3), pp. 155–163, 2012. (in Turkish)
https://doi.org/10.5505/pajes.2012.66375

[42] Cement Association of Canada (CSA) "Concrete Design Handbook", Cement Association of Canada, 2006. ISBN 1896553206

[43] Anıl, Ö., Ulusoy, B. "Nonlinear FEA of Two-Way RC Slabs' Punching Behavior of with Openings", Iranian Journal of Science and Technology, Transactions of Civil Engineering, 44(4), pp. 1109–1124, 2020.
https://doi.org/10.1007/s40996-019-00301-y

[44] Abdul Rasoul, Z. M. R. "Experimental Study of Punching Shear Strength of Self Compacting Concrete Slabs with Openings", Journal of Kerbala University, 9(2), pp. 88–100, 2011.

[45] Aguiar, A., Oliveira, D., Reis, L., Nzambi, A. "Punching shear strength of waffle flat slabs with opening adjacent to elongated columns", Engineering Structures, 243, 112641, 2021.
https://doi.org/10.1016/j.engstruct.2021.112641